View Online

Molecular BioSystems

www.molecularbiosystems.org

Volume 6 | Number 3 | March 2010 | Pages 425–604

Downloaded by University of Tennessee at Knoxville on 05 August 2011
Published on 10 December 2009 on http://pubs.rsc.org | doi:10.1039/B819206G

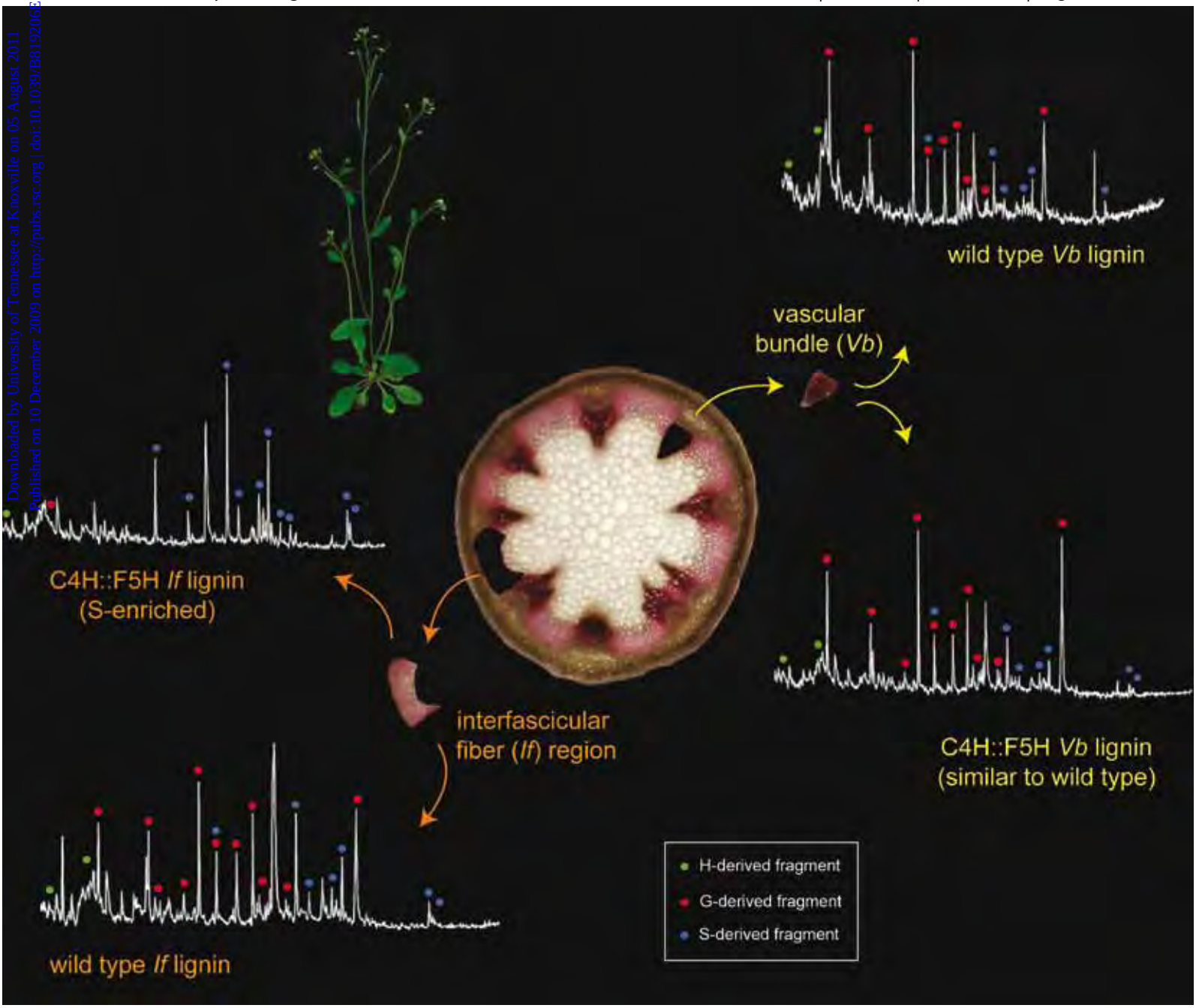

ISSN 1742-206X

RSC Publishing

PAPER

Ann M. Patten *et al.*

Probing native lignin macromolecular configuration in *Arabidopsis thaliana* in specific cell wall types: Further insights into limited substrate degeneracy and assembly of the lignins of *ref8*, *fah* 1–2 and C4H::F5H lines

View Online

Probing native lignin macromolecular configuration in *Arabidopsis thaliana* in specific cell wall types: Further insights into limited substrate degeneracy and assembly of the lignins of *ref8*, *fah* 1–2 and C4H::F5H lines

Ann M. Patten,[a] Michaël Jourdes,[a] Claudia L. Cardenas,[a] Dhrubojyoti D. Laskar,[a] Yoshihisa Nakazawa,[a] Byung-Yeoup Chung,[a] Vincent R. Franceschi,†[b] Laurence B. Davin[a] and Norman G. Lewis*[a]

Received 31st October 2008, Accepted 22nd October 2009
First published as an Advance Article on the web 10th December 2009
DOI: 10.1039/b819206e

Downloaded by University of Tennessee at Knoxville on 05 August 2011
Published on 10 December 2009 on http://pubs.rsc.org | doi:10.1039/B819206E

The interest in renewable, plant-derived, bioenergy/biofuels has resulted in a renaissance of plant cell-wall/lignin research. Herein, effects of modulating lignin monomeric compositions in a single plant species, *Arabidopsis*, are described. The earliest stage of putative "AcBr/Klason lignin" deposition was apparently unaffected by modulating *p*-coumarate 3-hydroxylase or ferulate 5-hydroxylase activities. This finding helps account for the inability of many other studies to fully suppress the reported putative levels of lignin deposition through monolignol biosynthesis manipulation, and also underscores limitations in frequently used lignin analytical protocols. The overall putative lignin content was greatly reduced (*circa* 62%) in a plant line harboring an H-(*p*-hydroxyphenyl) enriched lignin phenotype. This slightly increased H-monomer deposition level apparently occurred in cell-wall domains normally harboring guaiacyl (G) and/or syringyl (S) lignin moieties. For G- and S-enriched lignin phenotypes, the overall lignification process appeared analogous to wild type, with only xylem fiber and interfascicular fiber cells forming the S-enriched lignins. Laser microscope dissection of vascular bundles and interfascicular fibers, followed by pyrolysis GC/MS, supported these findings. Some cell types, presumably metaxylem and possibly protoxylem, also afforded small amounts of benzodioxane (sub)structures due to limited substrate degeneracy (*i.e.* utilizing 5-hydroxyconiferyl alcohol rather than sinapyl alcohol). For all plant lines studied, the 8-*O*-4′ inter-unit frequency of cleavable H, G and/or S monomers was essentially invariant of monomeric composition for a given (putative) lignin content. These data again underscore the need for determination of lignin primary structures and identification of all proteins/enzymes involved in control of lignin polymer assembly/macromolecular configuration.

Introduction

The renewed general interest in biofuels/bioenergy/bioproducts has re-invigorated much of plant science research, in particular that of plant cell wall formation. A major limiting factor in utilizing plant biomass for bioenergy/biofuels though is the recalcitrance of biomass, which in turn is currently considered as largely resulting from lignification/lignin deposition.[1] In this context, much remains to be learned about how lignin assembly and macromolecular lignin configuration are controlled *in vivo*;[1] lignins are, next to cellulose, Nature's most abundant organic substances in vascular land plants.

The recent availability of genetically altered lines of *Arabidopsis thaliana* provides an additional means to probe lignification wherein the effects of manipulating lignin compositions and contents can be comprehensively studied in the same organism (reviewed in Ref. 1–3). The advent and application of relatively novel microtechnologies, such as laser microdissection has also provided the opportunity to explore lignification in distinct cell-wall types of lignified tissue(s).[4–6]

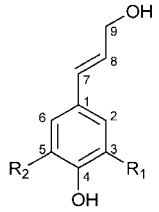

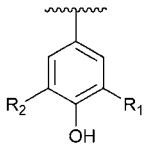

R_1=R_2=H, *p*-Coumaryl alcohol (**1**)
R_1=OMe, R_2=H, Coniferyl alcohol (**2**)
R_1=R_2=OMe, Sinapyl alcohol (**3**)
R_1=OMe, R_2=OH, 5-Hydroxyconiferyl alcohol (**4**)

R_1=R_2=H, *p*-Hydroxyphenyl (**H**) unit
R_1=OMe, R_2=H, Guaiacyl (**G**) unit
R_1=R_2=OMe, Syringyl (**S**) unit
R_1=OMe, R_2=OH, **5-OHG** unit

From an evolutionary perspective, lignification proper generally utilizes only three monomers, *i.e.* *p*-coumaryl (**1**), coniferyl (**2**) and sinapyl (**3**) alcohols, which differ simply in

[a] *The Institute of Biological Chemistry, Washington State University, Pullman, WA 99164-6340, USA. E-mail: lewisn@wsu.edu; Fax: +1 509-335-8206; Tel: +1 509-335-2682*
[b] *School of Biological Sciences, Washington State University, Pullman, WA 99164-4236, USA*
† Deceased.

View Online

Downloaded by University of Tennessee at Knoxville on 05 August 2011
Published on 10 December 2009 on http://pubs.rsc.org | doi:10.1039/B819206E

their degree of methoxylation; in grasses, these moieties may also be acylated to some extent.[7] Derived from the monolignols are the trivially described *p*-hydroxyphenyl (H), guaiacyl (G) and syringyl (S) lignins, respectively. Interestingly, lignin monomeric compositions, as well as their contents, can vary enormously between plant divisions (*e.g.* gymnosperms, angiosperms), as well as with cell types and subcellular layers.[7] This variability in lignin monomeric composition and/or derivatization does not shed any particular insight though into either how lignification occurs in cell walls of distinct cell types, or of the lignin macromolecular structures/configurations in distinct cell-wall layers that result.

In the overall study reported herein, three *Arabidopsis* lines modified in lignin monomeric compositions and contents were subjected to comprehensive analyses in order to begin to probe such questions further. These lines were the so-called *ref8*, *fah* 1–2, and C4H::F5H and contain H-, G- and S-enriched lignin phenotypes, respectively. The analyses included: plant growth/development profiles; histochemical and autofluorescence microscopy analyses of the vascular tissues; estimations of stem lignin monomeric compositions and amounts; laser capture microdissection (LCM) and pyrolysis GC/MS analyses of specific regions/cell types within the vasculature, as well as ^{13}C NMR spectroscopic analyses of both wild type (WT) and C4H::F5H lignin-enriched isolates.

As discussed below, the data obtained indicate that the lignin forming apparatus and thus control over lignin macromolecular configuration in different cell types and tissues were intactly maintained. Furthermore, the tissue specificity of S-lignin deposition in the various cell types was *not* abolished in the C4H::F5H line, as had previously been reported to occur by Meyer *et al.*[8] Indeed, the results from some of the analyses in the current studies again underscore the inherent limitations of studying "averaged" lignin compositions from different cell/tissue types rather than the individual cell wall types from which they were derived. Additionally, the question of metabolic plasticity/combinatorial chemistry in lignification,[9] can now instead be considered as resulting from a very limited form of substrate degeneracy during proposed template polymerization[10–13] in individual cell (wall) types. An alternate viewpoint of lignification (random/combinatorial chemistry) is discussed elsewhere,[9,14] the content of much of which has been systematically and critically addressed.[1]

Results

Phenotype differences in stem growth and development

It was first instructive to compare the overall (stem) growth and developmental patterns of the WT (ecotype Columbia), *ref8*, *fah* 1–2 and C4H::F5H *Arabidopsis* lines. This was in order to evaluate gross effects of the various genetic modifications throughout stem growth, including into late maturity. By contrast, numerous other investigations have over-looked progressive growth/developmental changes and have based conclusions on a single developmental stage (critically discussed in Ref. 2, 15–17). Thus, the comparative analyses of both stem lengths and widths, as a function of time (Fig. 1a and b), showed that at least two of the *Arabidopsis*

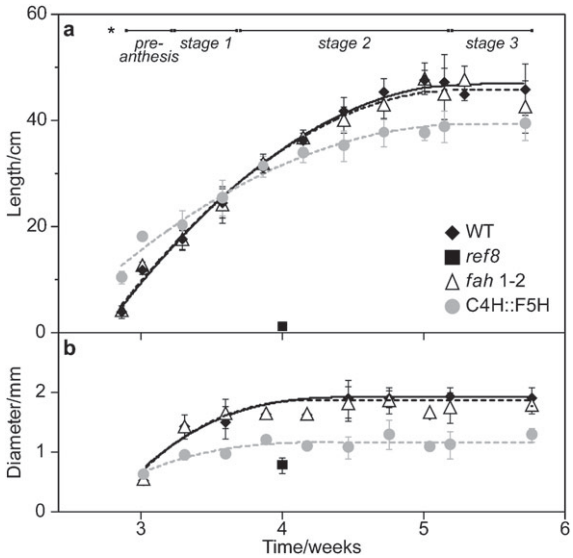

Fig. 1 Lengths (a) and diameters (b) of stem growth of WT, *ref8*, *fah* 1–2 and C4H::F5H *Arabidopsis* lines over time. For reference to discussion of histochemical results, stages of reproductive growth (*)[20] are shown as approximate time intervals and are based on WT development. See text for variations recorded for C4H::F5H and *ref8* development.

lines (*ref8* and C4H::F5H) were greatly affected, relative to WT, *i.e.* as previously noted for the CCR1 *irx4* mutant.[17] The *ref8* was severely stunted[18,19] as demonstrated by large reductions in both stem lengths and widths (~2.4 cm and ~0.8 mm, respectively) at 4 weeks of growth and development, when compared to the WT (~31 cm and ~1.6 mm, respectively; ■, ◆ Fig. 1a and b). The C4H::F5H stem length was initially almost twice as long as WT (~3 weeks), but stem thickness was *circa* 30% less, irrespective of growth/developmental stage. However, subsequent C4H::F5H growth (>3 weeks) was gradually reduced and resulted in a shorter stem length on average. This unusual stem growth apparently affected overall physiology, leading to early senescence in C4H::F5H relative to WT (data not shown). This occurred despite C4H::F5H having reached its maximum height at approximately the same time (~5 weeks) as WT (●, ◆, Fig. 1a). The *fah* 1–2 line, however, was very similar to that of WT as shown by nearly identical stem length and width measurements as a function of time (△, ◆, Fig. 1).

Morphology and histochemical comparisons

The various results herein are reported in the context of *Arabidopsis* anatomical descriptors developed by Altamura *et al.*[20] In that earlier investigation, a detailed comparison of *Arabidopsis* stem vasculature within reproductive development (both Columbia and Wassilewskija ecotypes) was made for the purpose of aiding comparison between WT and genetically-altered lines; the latter can vary greatly in size and timing of development.[20] In brief, stages of vascular development were described in relation to anthesis of the first flower, *i.e. pre-anthesis* (early vascular bundles present, differentiated interfascicular fibers (*ifs*) absent), *stage 1* (first silique differentiated; early

 This journal is © The Royal Society of Chemistry 2010

View Online

development of secondary walls in *ifs*); *stage 2* (immature siliques and apical buds present; deposition of lignin in *ifs*) and *stage 3* (all siliques dehiscent, few apical buds present; continuous vascular structure/cambium found throughout the stem).

In the current study, comparison of morphological and histochemical (lignin) features demonstrated a close correlation between stem growth phenotype and anatomy/lignin histochemistry. The *ref8* line was most striking, with severe collapse of the metaxylem (*mx*, Fig. 2d). The latter had also been noted by Franke *et al.*[19] For the C4H::F5H line, early accelerated stem elongation and reduced stem width (●, Fig. 1), correlated to an overall smaller vascular system, with some early metaxylem showing an altered anatomy with irregular cell walls (*mx*, Fig. 2c, g and j). Similar quantitative stem length and width values, observed for WT and *fah* 1–2 over time (△, ◆, Fig. 1), were qualitatively reflected in the stem vascular anatomies of both lines at 4 weeks or *stage 2*[20] (Fig. 2a and b).

Downloaded by University of Tennessee at Knoxville on 05 August 2011
Published on 10 December 2009 on http://pubs.rsc.org | doi:10.1039/B819206E

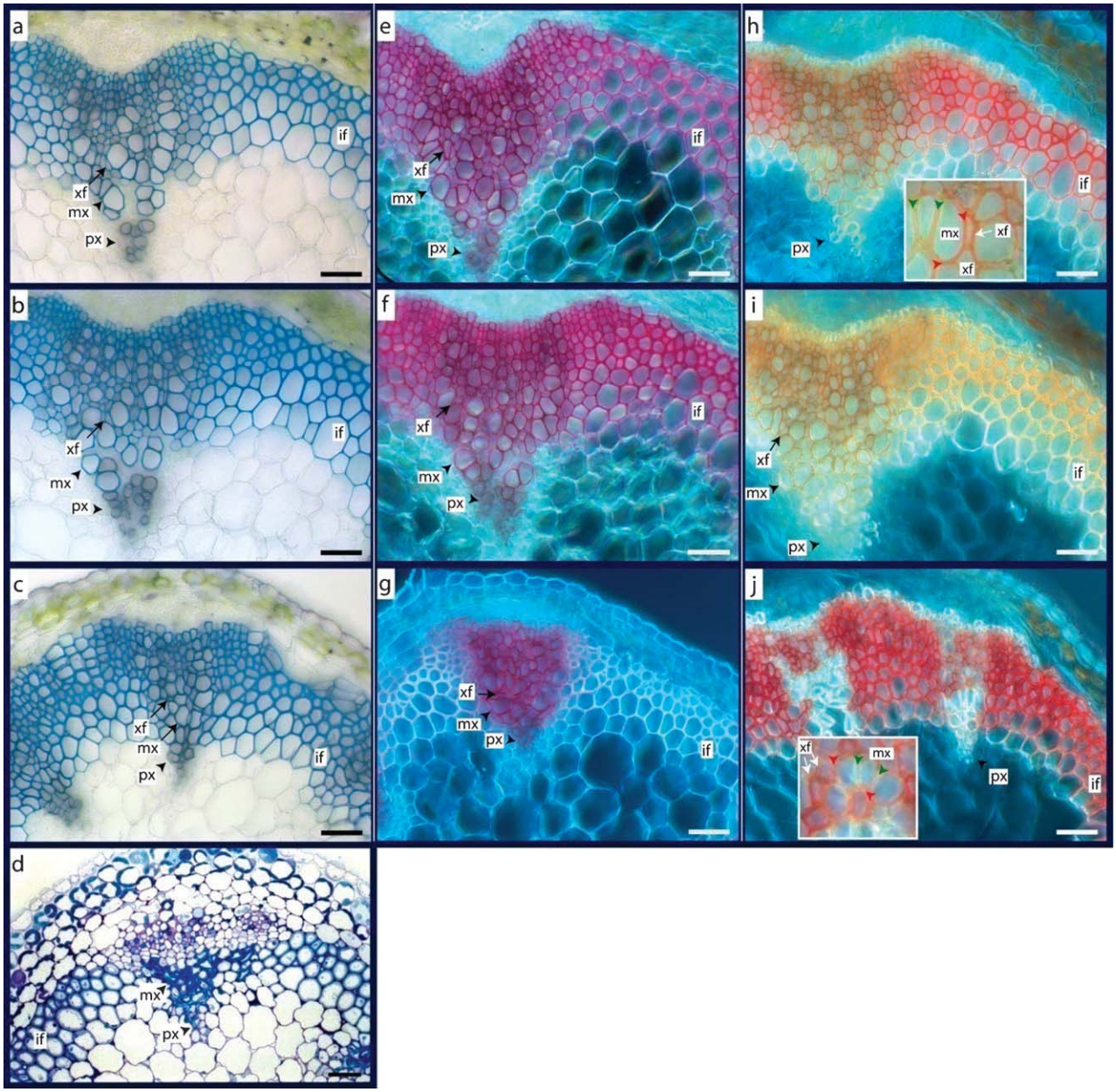

Fig. 2 General anatomy (a–d) and lignin histochemical properties (e–j) of *Arabidopsis* lines WT (a,e,h), *fah* 1–2 (b,f,i), C4H::F5H (c,g,j) and *ref8* (d) at *stage 2* of reproductive growth.[20] Most notably, the *ref8* had severely collapsed *mx* (d). Specific histochemistries to detect presumed coniferyl alcohol (**2**)-derived moieties by phloroglucinol-HCL (red-purple color; e–g) and sinapyl alcohol (**3**)-derived moieties by the Mäule reaction (red color; h–j) suggested that WT and *fah* 1–2 anatomies were very similar (e, f), except for *fah* 1–2 lacking S-lignin (i). CH4::F5H had reduced G-lignin in *if* cell walls (g) and apparent overexpression of S-lignin in both *if* and *xf* cells (j). Moreover, within the vascular bundle in both WT and the C4H::F5H, Mäule reagent reactivity is specific to *xf* cell walls (see Results section). Images were recorded using brightfield (a–d) or Nomarski illumination (e–j). Scalebars: 25 μm (d); 50 μm (a-c, e–j). Abbreviations: *if*, interfascicular fiber; *mx*, metaxylem; *px*, protoxylem; *xf*, xylary fibers.

View Online

Downloaded by University of Tennessee at Knoxville on 05 August 2011
Published on 10 December 2009 on http://pubs.rsc.org | doi:10.1039/B819206E

Lignin staining

Histochemical staining of the presumed G (coniferyl alcohol-derived) lignin moieties was carried out using phloroglucinol-HCl[21,22] with fresh hand-cut sections taken near the base of the stem. The red histochemical staining of the presumed G moieties that so resulted was readily detected in the *mx* and xylary fibers (*xf*) of the WT, *fah* 1–2, and C4H::F5H vascular bundles at 4 weeks/*stage 2*[20] (*mx*, *xf*, Fig. 2e–g). Red staining was, however, less visible in the protoxylem (*px*) possibly due to three factors: (1) the *px* annual to spiral secondary cell wall thickenings do not lie fully parallel to the transverse section; (2) some *px* walls are crushed during normal development of the *mx*,[23] and are thus not fully accessible to the reagent; and (3) *px* may have either low to no levels of G-lignin present (discussed later).

With this reagent, presumed G-lignin moieties were detected in the neighbouring interfascicular fiber (*if*) regions of WT and *fah* 1–2 (Fig. 2e and f), but only very faintly in those of the C4H::F5H line (Fig. 2g). In addition to the results shown for 4 weeks/*stage 2*,[20] phloroglucinol–HCl staining experiments using plants at 5 and 7 weeks (late *stage 2* and *stage 3*,[20] respectively) further demonstrated that the observed patterns of presumed G-lignin deposition remained consistent in the three lines over time (data not shown). No clear assessment of lignin deposition patterns using histochemistry was possible with the *ref8* tissue due to its structural fragility; these methods stain fresh, non-fixed, specimens under quite harsh chemical conditions and which resulted in near dissolution of the sections when using the *ref8* tissue.

Differential histochemical detection of the S-lignin was also conducted using the Mäule[24] reagent. For WT tissue, a presumed S-lignin (dark red coloration) was clearly evident in the *if* and *xf* cells (Fig. 2h and inset). By contrast, the *mx* stained yellow to brown with this reagent, indicative of mostly G-lignin being present.[25–27] It should be noted that Mäule staining of the vascular bundle resulted in partial red coloration of *mx* where these cell walls are in direct contact with the Mäule reagent-positive *xf* cells (red arrowheads of Fig. 2h inset). This apparent *mx* reactivity may be either an artifact of reagent carry-over from the *xf* cells (light microscopy lacks sufficient resolution to differentiate individual cell walls) or partial diffusion of S-monolignols to the adjacent *mx* cell walls. In any case, the *mx* cell walls do not themselves appear to generate S-lignin as noted in the light brown coloration where *mx* cell walls adjoin (green arrowheads of Fig. 2h inset). Additionally, the *fah* 1–2 genotype showed no obvious S-lignin moieties in any cell type (Fig. 2i), this presumably corresponding to their near absence in this plant line (see later). Given the overall similarity of *fah* 1–2 to WT in terms of growth (Fig. 1) and general anatomy (Fig. 2b/f and a/e, respectively), it is possible that the *fah* 1–2 lignin functions in a physiologically similar way to that of "normal" cell wall lignins in gymnosperms; gymnosperms do not typically synthesize S-lignin moieties (reviewed by Gibbs[26]).

Conversely, the *if* and *xf* cells of the C4H::F5H line appeared S-lignin-positive (Fig. 2j and inset) as qualitatively found in WT. The C4H::F5H *mx* cell walls differentially stained a very light brown coloration (green arrowheads of Fig. 2j inset), again as in WT, with an apparent slight carry-over of red coloration where *mx* cell walls are directly in contact with *xf* cell walls (red arrowheads of Fig. 2j inset). In general though the light brown coloration of the *mx* cell walls suggest the deposition of predominantly G, and perhaps also 5-OHG, moieties due to potential F5H overexpression in these particular cells (discussed later). Additionally, no S-lignin was detected in the *px* cell walls. Mäule histochemistry was also conducted using these lines at 5 and 7 weeks (late *stage 2* and *stage 3*,[20] respectively); the same localization patterns were found, indicating consistent deposition of S moieties in the lignin in these cell wall types over time (data not shown).

Ultraviolet microscopy (UV) lignin/phenolic detection by autofluorescence

Autofluorescence of developing and mature lignified cells was also examined using *stage 2*[20] stems (Fig. 3). In all cases, the fluorescence inherent to presumed lignin/phenolics was detected in protoxylem (*px*), metaxylem (*mx*) and interfascicular fiber (*if*) cell walls, in agreement with lignin histochemistry results (complete data not shown). For example, developing *if* cells (*if'*) in WT and *fah* 1–2 showed intense autofluorescence in the cell wall corners of *if'*(*cwc2*), with lignification throughout the cell walls of mature *if* cells (*L2*, *if*, Fig. 3a and b). Similar developmental patterns were visible in the C4H::F5H and *ref8 mx* (cell wall corners of *mx*, *cwc1*; lignifying cell walls of *mx*, *L1*; Fig. 3c and d). In the case of C4H::F5H, areas of intense autofluorescence were present in the *xf* (Fig. 3c), which may correspond to Mäule histochemical results (Fig. 2j) and enhanced S-lignin deposition detection.

Interestingly, intense autofluorescence was present in the *mx* of *ref8* (Fig. 3d), this apparently being due to collapse and compression of the *mx* cell walls. Autofluorescence in the *cwc2* may correspond to early H-lignin deposition and appears distinctly brighter than in the lateral *if* cell walls (*L2*, Fig. 3d). The *ref8 L2* autofluorescence (Fig. 3d) also appears less intense than that of WT (Fig. 3a), suggesting overall reduced lignification in the *ref8 if* region. As noted aforehand, this is expected as *ref8* is strongly reduced in G and S lignin contents and would be anticipated to particularly affect the secondary cell walls (*sw*), as angiosperm *sw* are often composed primarily of S lignin with lesser amounts of G lignin. Taken together, the overall sequence of lignin macromolecular assembly in distinct cell layer regions/cell wall types appeared to be relatively unchanged, except in the case of the *ref8* line, which is much less lignified (discussed below).

Estimated putative lignin contents and monomeric compositions at early phases of vascular development

Given the findings obtained with histochemical and autofluorescence analyses, it was next deemed instructive to examine the question of putative lignin deposition at a very early stage of vascular development (pre-anthesis). To do this, tissues enriched in *px* cell walls were isolated from very young stems of WT plants (*circa* 1 cm long) still undergoing elongation (*i.e.* essentially involving primary growth and *px* development only, *stage 1*[20]) (Fig. 4). The estimated/putative lignin and/or (poly)phenolic contents of such tissues were low at this stage

 This journal is © The Royal Society of Chemistry 2010

View Online

Downloaded by University of Tennessee at Knoxville on 05 August 2011
Published on 10 December 2009 on http://pubs.rsc.org | doi:10.1039/B819206E

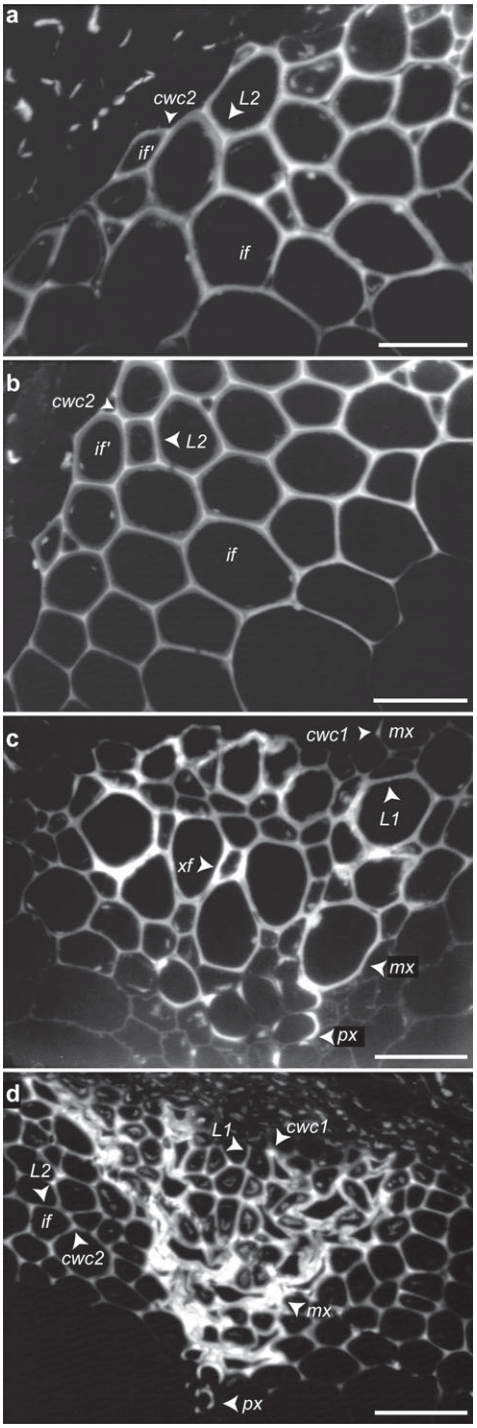

Fig. 3 Lignin autofluorescence in WT (a) and *fah* 1–2 (b) interfascicular fibers and in C4H::F5H (c) and *ref8* (d) xylem regions. Scale bars: 25 μm. Abbreviations: see Results section.

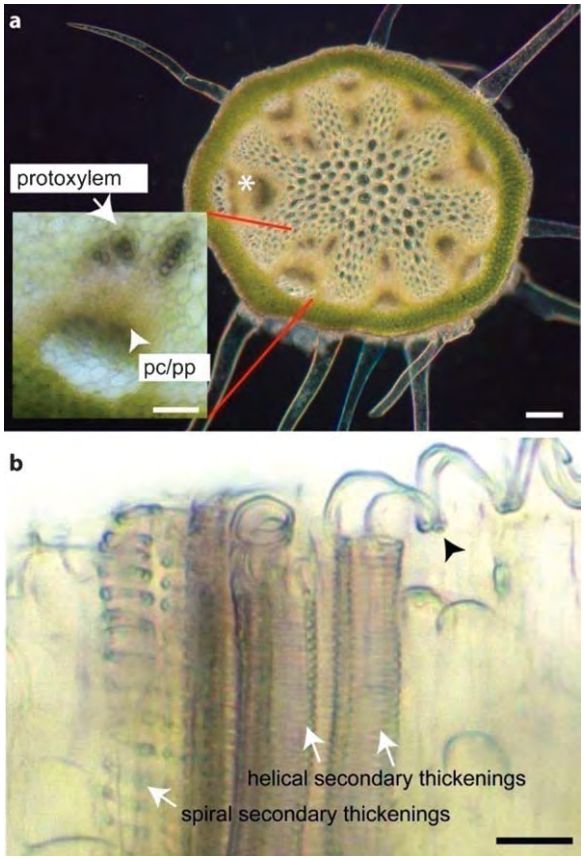

Fig. 4 Protoxylem in *Arabidopsis* wild type as an example of tissue used for estimation of lignin contents and monomeric compositions. The protoxylem (*px*) of such young stems appear as small isolated bundles in cross-section (a and inset for a), but natural variability also occurs wherein one or two vascular bundles may be more developed with both *px* and metaxylem (*mx*) (*). In longitudinal sections, *px* elements are recognizable by their spiral to helical secondary cell wall thickenings that are highly extensible to allow for stem elongation during primary growth; this extensibility is demonstrated by preparation artifact (black arrowhead). Scale bars are 100 μm (a) and 10 μm (b). Abbreviation: pc/pp, procambial/protophloem region.

of development [*i.e.* for the WT line, the 'AcBr lignin' content was *circa* 6% cell wall residue (CWR), relative to that of *circa* 20% at maturation, see Table 1].

Alkaline nitrobenzene oxidation (NBO) and thioacidolysis chemical degradation techniques were applied to these *px*-enriched tissues as well. In angiosperms, the alkaline NBO method can cleave C_7–C_8 bonds in lignins *and* other phenolics to release *p*-hydroxybenzaldehyde (**5**), vanillin (**6**) and syringaldehyde (**7**), as well as the corresponding *p*-hydroxybenzoic acid moieties (**8–10**). Thioacidolysis, by contrast, releases the corresponding monomeric products **11–13**, this being considered to mainly occur through 8-*O*-4′ interunit bond cleavage of lignins. For the thioacidolysis analyses, the liberated monomeric entities (~8.6 μmol g^{-1} CWR) were largely, but not exclusively, of H-character with smaller amounts of G being released as well (Table 1). Somewhat analogous results were obtained for NBO determinations as well.

Additionally, *px*-enriched cell wall preparations from the four plant lines (WT, *ref8*, *fah* 1–2 and C4H::F5H) were subjected to pyrolysis GC/MS (data not shown). Analysis of the resulting pyrograms again indicated the presence of largely H-related moieties. Interestingly, however, proteomic analysis of protoxylem (*px*) gave preparations lacking in monolignol biosynthetic pathway enzymes (data not shown) suggesting

View Online

Downloaded by University of Tennessee at Knoxville on 05 August 2011
Published on 10 December 2009 on http://pubs.rsc.org | doi:10.1039/B819206E

Table 1 Estimations of lignin amounts and cleavable monomeric entities at different developmental stages of *Arabidopsis* WT, *ref8*, *fah* 1–2 and C4H::F5H lines

	Plant lines					
		WT		*ref8*	*fah* 1–2	C4H::F5H
Growth stage		*Pre-anthesis of 1st flower*[20] (~1 cm stem)	*Stage 3*[20]	*Stage 3*[20]	*Stage 3*[20]	*Stage 3*[20]
Biochemical step modulation		None	None	*p*C3H mutation	F5H mutation	F5H over-expression
Estimated lignin content (% CWR)	Klason	5.9 ± 0.5	20.6 ± 0.4	7.8 ± 0.8	23.1 ± 0.9	17.0 ± 0.6
	AcBr	6.1 ± 0.1	19.8 ± 0.5	ne[a]	21.2 ± 0.4	17.1 ± 0.3
Thioacidolysis (μmoles g^{-1} of CWR)	H	7.2 ± 0.5	2.9 ± 0.1	ne	3.1 ± 0.2	4.3 ± 0.1
	G	1.4 ± 0.2	198.6 ± 7.2	ne	292.6 ± 9.7	6.6 ± 0.4
	S	nd[b]	53.6 ± 1.4	ne	nd	176.6 ± 9.3
	Total	8.6 ± 0.6	255.1 ± 9.5	ne	295.7 ± 10.2	187.5 ± 10.2
	H : G : S	84 : 16 : nd	1 : 78 : 21	ne	1 : 99 : nd	2 : 4 : 94
	Yield of putative lignin (%)	2	26	ne	27	26
Alkaline NBO (μmoles g^{-1} of CWR)	H	11.9 ± 0.7	5.6 ± 0.7	64.7 ± 0.8	4.2 ± 0.2	4.6 ± 0.5
	G	7.3 ± 0.4	214.3 ± 6.6	14.8 ± 0.4	285.9 ± 8.6	14.3 ± 0.8
	S	nd	55.4 ± 3.3	5.1 ± 0.3	nd	197.9 ± 7.3
	Total	19.2 ± 0.9	275.3 ± 8.2	84.6 ± 1.5	290.1 ± 10.1	216.8 ± 9.5
	H : G : S	62 : 38 : nd	2 : 78 : 20	77 : 17 : 6	1 : 99 : nd	2 : 7 : 91
	Yield of putative lignin (%)	6	28	21	27	28

[a] ne: not estimated. [b] nd: not detected.

involvement of other phenolic types interfering with the lignin analysis (see Fig. 5).

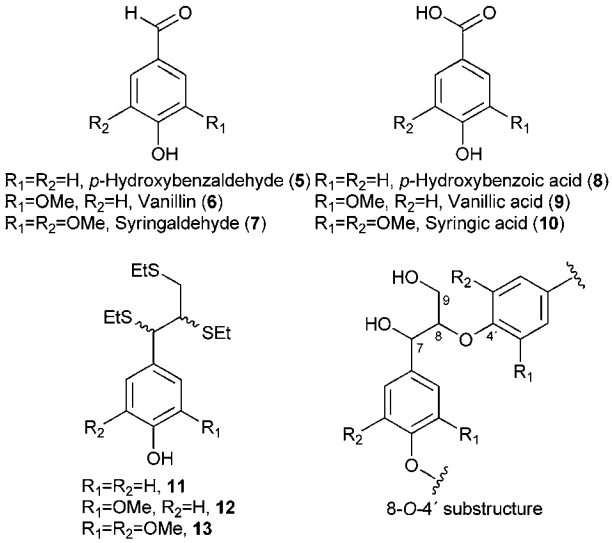

Estimated lignin contents and monomeric compositions at maturation

Attention was next directed to a comprehensive analysis of the various *Arabidopsis* lines at maturation (*stage 3*[20]) in order to gain further insight into how lignification was either conserved and/or perturbated in distinct cell wall types.

ref8. Detailed lignin analyses were carried out to investigate whether the *p*C3H mutation resulted in any definitive separation of the presumed distinct phases of H and G(S) lignin formation. The estimated/putative lignin contents of *ref8* at stem maturation were found to be markedly reduced relative to WT (~7.8 *vs.* ~20.6%) (Table 1), as suggested by the Klason lignin method. That the cleavable monomers within the presumed *ref8* lignin were apparently mainly of an H-character was indicated from results obtained using alkaline NBO (Table 1) and pyrolysis GC/MS analyses (Fig. 6).

From the alkaline NBO data, the monomeric H : G : S ratio for *ref8* was estimated to be ~77 : 17 : 6 *vs.* that of ~2 : 78 : 20 for WT, with overall recoveries of cleavable monomers (based on their estimated lignin contents) of *circa* 21 and 28%, respectively. This mutated line also liberated small amounts of both G and S cleavable monomeric components.

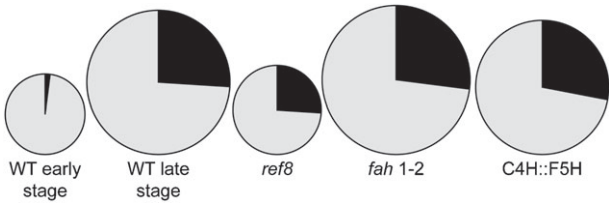

Fig. 5 Comparative estimated/putative lignin contents *versus* extractive free CWR dry weight [represented by complete circle areas of corresponding size for *ref8*, *fah* 1–2, C4H::F5H and WT (early and late developmental stages) lines]. Data are normalized against lignin levels at maturation of the WT line; areas shaded in black correspond to quantification of alkaline NBO and/or thioacidolytic released monomers.

 This journal is © The Royal Society of Chemistry 2010

View Online

Downloaded by University of Tennessee at Knoxville on 05 August 2011
Published on 10 December 2009 on http://pubs.rsc.org | doi:10.1039/B819206E

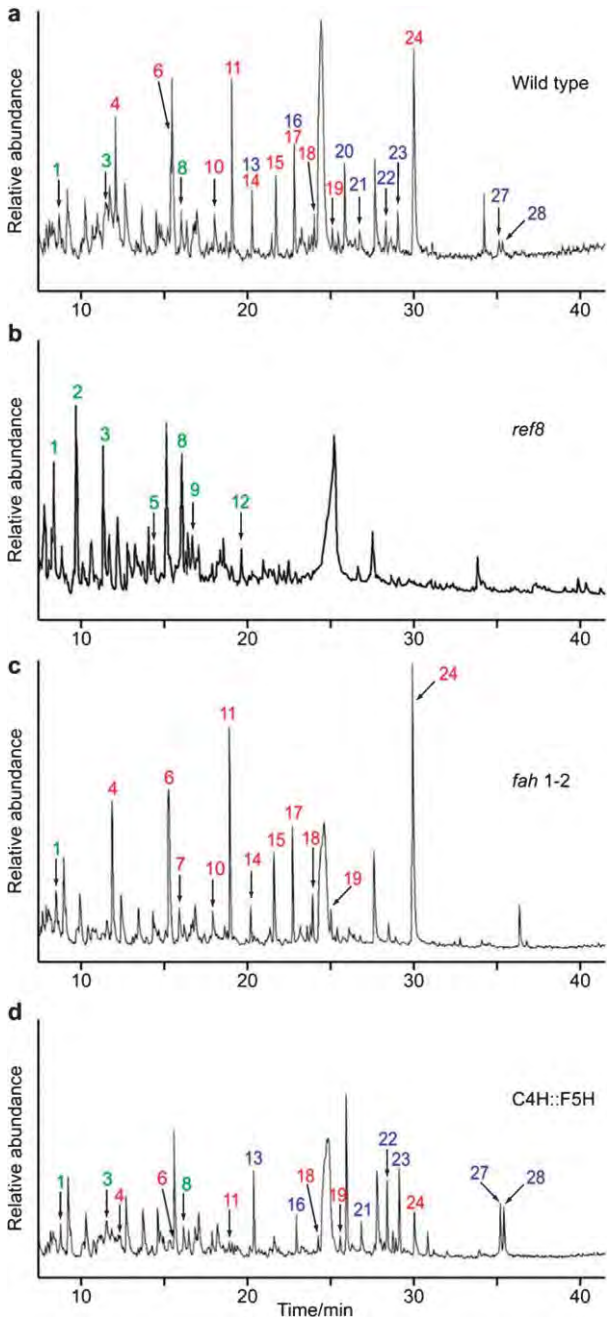

Fig. 6 Pyrolysis GC/MS of mature (*i.e. stage 3* of reproductive growth[20]) WT, *ref8*, *fah* 1–2 and C4H::F5H *Arabidopsis* stem cell wall residues (CWRs).

Pyrolysis GC/MS of the *ref8* stem tissue, however, gave a pyrogram whose major peaks detected were the putative H-lignin-derived components, namely phenol (peak 1), 4-methylphenol (peak 2), 3-methylphenol (peak 3), 4-ethylphenol (peak 5), 4-vinylphenol (peak 8), 4-allylphenol (peak 9) and *trans*-4-propenylphenol (peak 12) (Fig. 6b and Table 2[28,29]). By contrast to the alkaline NBO analyses, however, there were no readily detectable G and S monomeric derived entities, at least down to the baseline level of detection employed.

Pyrolysis GC/MS of mature WT stem tissue, by comparison, afforded presumed lignin-derived components that were mainly of G- (peaks 4, 6, 10, 11, 14, 15, 17–19 and 24) and S- (peaks 13, 16, 20–23, 27 and 28) character, together with comparatively lower amounts of the H-derived components (peaks 1, 3 and 8) being detected (see Fig. 6a and Table 2).

Effects of manipulating F5H on cell wall-specific lignin macromolecular assembly and configuration

The estimated lignin contents and monomeric compositions for the WT, *fah* 1–2 and C4H::F5H lines at maturation (7 weeks/*stage 3*[20]) are also summarized in Table 1. Stems of the three plant lines were first subjected to AcBr lignin analyses, with these being proportionally estimated based on their presumed H : G : S monomeric compositions and individual extinction coefficients for H, G and S-enriched lignin preparations. [In this regard, our current best estimates for the extinction coefficients for H, G and S-enriched lignin isolation are ~15.31, 18.61 and 14.61 l g^{-1} cm^{-1}, respectively, for *Arabidopsis*.[16]] Using these values at present, the WT, *fah* 1–2 and C4H::F5H CWRs were thus provisionally calculated to have estimated lignin contents of ~19.8, ~21.2 and ~17.1%, respectively, based on the presumed monomeric composition/AcBr analyses (Table 1).

The H : G : S monomeric compositions were estimated based on both thioacidolysis cleavage/alkaline NBO degradative analyses of the CWRs for each of the three lines. For the WT line, the H : G : S ratio of thioacidolytically cleaved monomers released was 1 : 78 : 21, with the total amount quantified as ~255 μmol g^{-1} CWR. However, on a percentage basis, this accounts for only *circa* 26% of the presumed lignin present. Somewhat comparable results were obtained using NBO degradation (275 μmol g^{-1} CWR, 28% of estimated/putative lignin content).

For the *fah* 1–2 line, the 'AcBr lignin' content was estimated to be fractionally higher (~21.2%), with an H : G ratio of 1 : 99 and a quantifiable total monomer release of ~296 μmol g^{-1} CWR. This cleavable monomeric release was *circa* 27% of the presumed lignin content. No S moieties were detected, however, at least down to the baseline levels of detection used in this study. This was further supported by pyrolysis GC/MS analysis of the *fah* 1–2 CWR which only detected the presence of G (peaks 4, 6, 7, 10, 11, 14, 15, 17–19 and 24), and H (peak 1) lignin-derived moieties (Fig. 6c).

For the C4H::F5H line, the estimated 'AcBr lignin' contents were somewhat lower (~17.1% of CWR), with an apparent H : G : S monomer ratio of 2 : 4 : 94 and a quantifiable (thioacidolysis cleavable) monomer release of ~188 μmol g^{-1} CWR (Table 1). This amount of cleavable monomers represents *circa* 26% of the putative lignin, this being near equivalent to the cleavable monomer yields for either the WT or *fah* 1–2 lines, when normalized for estimated lignin content. Alkaline NBO oxidation also gave somewhat comparable results (~28% of putative lignin content). Additionally, all three H, G and S presumed lignin-derived moieties were detected using pyrolysis GC/MS (Fig. 6d) as follows: H-derived units (peaks 1, 3 and 8), G-derived units (peaks 4, 6, 11, 18, 19 and 24), and S-derived moieties (peaks 13, 16, 21–23, 27 and 28).

View Online

Downloaded by University of Tennessee at Knoxville on 05 August 2011
Published on 10 December 2009 on http://pubs.rsc.org | doi:10.1039/B819206E

Laser microscopy dissection of WT, *fah* 1–2 and C4H::F5H interfascicular fiber (*if*) and vascular bundle regions

To gain additional insight into how lignification was affected at the single cell/specific tissue level, laser microscope dissections of basal cross-sections of mature stems (*stage 3*[20]) of WT, *fah* 1–2 and C4H::F5H lines were next carried out (see Fig. 7 for an example using WT tissues), with the resulting interfascicular fiber (*if*) and vascular bundle regions from each line individually subjected to pyrolysis GC/MS analyses (Fig. 8).

Interfascicular fibers

For the WT tissue, the pyrolysis GC/MS data established the presence of presumed H- (peaks 1 and 3), G- (peaks 4, 6, 7, 1

Table 2 Pyrolysis GC/MS identification of putative phenolic products according to Ref. 28 and 29

Peak number	Compound	Unit	Ions
1	Phenol	H	94, 66
2	4-Methylphenol	H	108, 107, 90, 77
3	3-Methylphenol	H	108, 107, 90, 79, 77
4	Guaiacol	G	124, 109, 81, 53
5	4-Ethylphenol	H	122, 107, 77
6	4-Methylguaiacol	G	138, 123, 95, 77, 67
7	Catechol	G[a]	110, 92, 81, 64, 63
8	4-Vinylphenol	H	120, 109, 91, 65
9	4-Allylphenol	H	134, 133, 107, 77
10	4-Ethylguaiacol	G	152, 137, 122
11	4-Vinylguaiacol	G	150, 135, 107, 77
12	*trans*-4-propenylphenol	H	134, 133, 107, 105, 77
13	2,6-Dimethoxyphenol	S	154, 139, 111, 96, 65
14	Eugenol	G	164, 149, 133
15	Vanillin	G	152, 151, 137, 123, 109
16	2,6-Dimethoxy-4-methylphenol	S	168, 121, 93, 65
17	*trans*-isoeugenol	G	164, 149, 131, 103, 77
18	Acetovanillone	G	166, 151, 123
19	Guaiacylacetone	G	180, 137, 122
20	2,6-Dimethoxy-4-vinylphenol	S	180, 165, 137, 122
21	4-Allyl-2,6-dimethoxyphenol	S	194, 179, 147, 119
22	Syringaldehyde	S	182, 153, 139, 111, 96
23	*trans*-2,6-dimethoxy-4-propenylphenol	S	194, 179, 151, 131
24	*trans*-coniferyl alcohol	G	180, 137, 124
25	Acetosyringone	S	196, 181, 153, 138, 93, 67
26	Syringylacetone	S	210, 167, 123, 69
27	*trans*-sinapyl aldehyde	S	208, 180, 177, 165, 137
28	*trans*-sinapyl alcohol	S	210, 167, 154, 107

[a] Possibly G-derived.

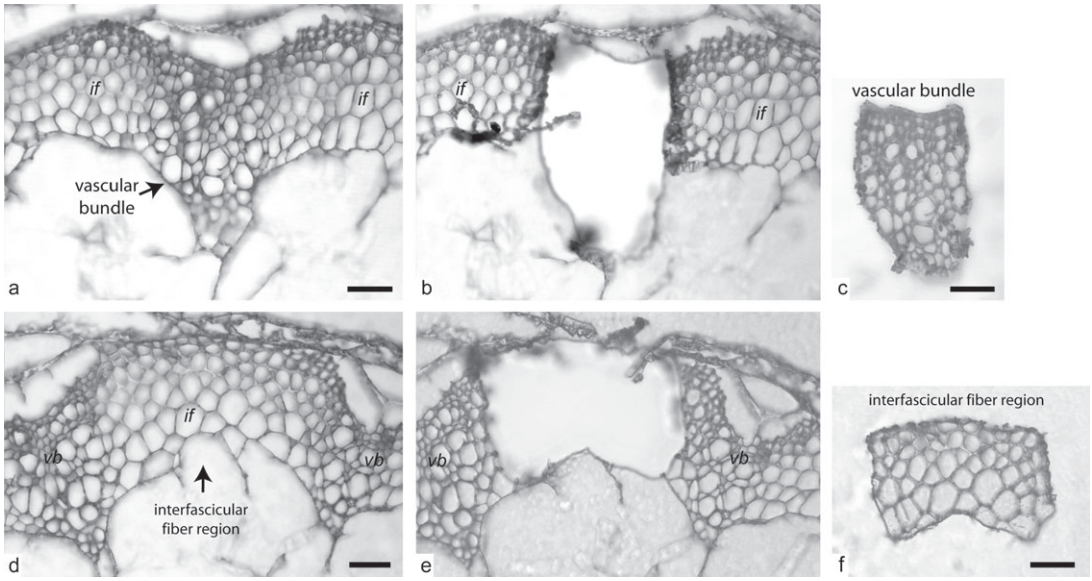

Fig. 7 An example of laser capture microdissection of *Arabidopsis*. Vascular bundles (a) were laser excised (b) and isolated (c), as were the interfascicular fiber (*if*) regions (d–f) from the base of a WT inflorescence stem. All scale bars are 50 μm.

 This journal is © The Royal Society of Chemistry 2010

View Online

Downloaded by University of Tennessee at Knoxville on 05 August 2011
Published on 10 December 2009 on http://pubs.rsc.org | doi:10.1039/B819206E

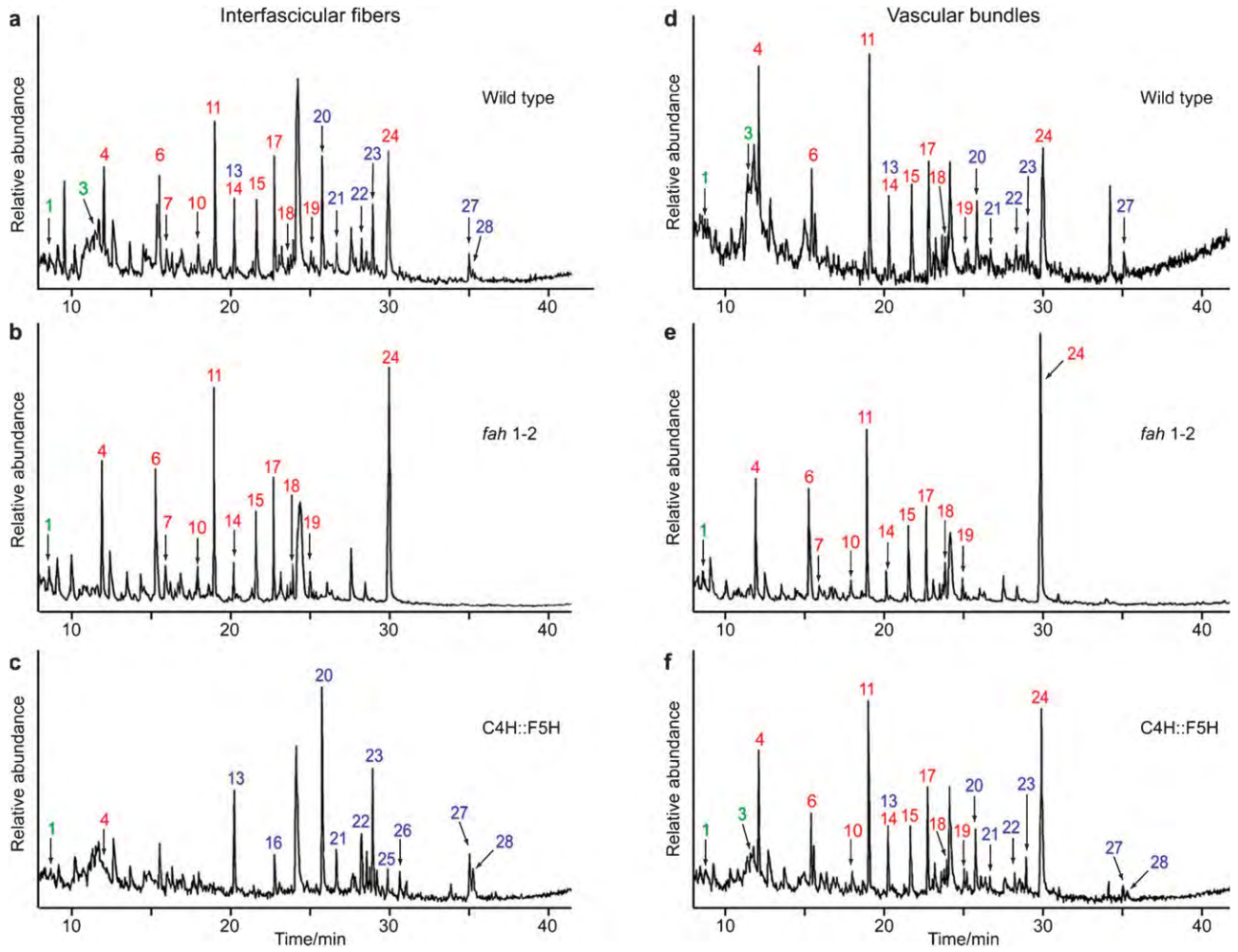

Fig. 8 Pyrolysis GC/MS of CWR of interfascicular fibers (a–c) and vascular bundles (d–e) isolated from the base of WT, *fah* 1–2 and C4H::F5H *Arabidopsis* stems (*i.e. stage 3* of reproductive growth[20]).

0, 11, 14, 15, 17–19 and 24) and S- (13, 20–23, 27 and 28) lignin derived moieties (see Fig. 8a and Table 2).

The *fah* 1–2 tissue, however, gave a pyrolysis GC/MS chromatogram (Fig. 8b) that now only contained small amounts of presumed H- (peak 1) and mainly G- (peaks 4, 6, 7, 10, 11, 14, 15, 17–19 and 24) lignin derived units; no S-units were detectable. On the other hand, the C4H::F5H tissue gave a chromatogram mainly containing S-derived moieties (peaks 13, 16, 20–23, and 25–28), as well as small peaks corresponding to H (peak 1) and traces of G (peak 4) moieties (Fig. 8c).

Vascular bundles

As indicated earlier, these contain *px*, *mx* and *xf* cells, with the first two cell wall types putatively harboring H/G-lignins and the latter H/G/S-derived lignins in the WT line. In potential agreement with this assumption, pyrolysis GC/MS of the WT vascular bundle tissue (Fig. 8d and Table 2) demonstrated the presence of presumed H- (peaks 1 and 3), G- (peaks 4, 6, 11, 14, 15, 17–19, and 24) and S- (peaks 13, 20–23 and 27) lignin-derived moieties, respectively.

The *fah* 1–2 vascular bundles, however, next provided a chromatogram lacking S-units (Fig. 8e), and is mainly of an H/G character (H-derived entities, peak 1; G-derived, peaks 4, 6, 7, 10, 11, 14, 15, 17–19 and 24).

The C4H::F5H vascular bundle tissue, by contrast, afforded a pyrolysis GC/MS chromatogram (Fig. 8f) very similar to that of WT tissue, namely containing H- (peaks 1 and 3), G- (peaks 4, 6, 10, 11, 14, 15, 17–19 and 24), and S- (peaks 13, 20–23, 27 and 28) lignin derived moieties.

The *px* and *mx* cells in C4H::F5H might be anticipated to have generated, at least in part, 5-OHG moieties rather than G. This is based on the assumption that the so-called caffeic acid *O*-methyltransferase (COMT), which *O*-methylates only 5-OHG moieties *in vivo*,[30] is not expressed in these cell types. If this occurs, the presence of an additional 5-OHG group would predictably affect the programmed lignification response, *i.e.* due to its hydroxyl group serving as an internal nucleophile post-coupling (Fig. 9) (see discussions in Ref. 1–3). Accordingly, limited substrate versatility could lead to formation of benzodioxane substructures as shown. At present, however, detection of putative benzodioxane substructures cannot currently be established using either pyrolysis GC/MS, thioacidolysis and/or alkaline NBO degradation analyses.

View Online

Downloaded by University of Tennessee at Knoxville on 05 August 2011
Published on 10 December 2009 on http://pubs.rsc.org | doi:10.1039/B819206E

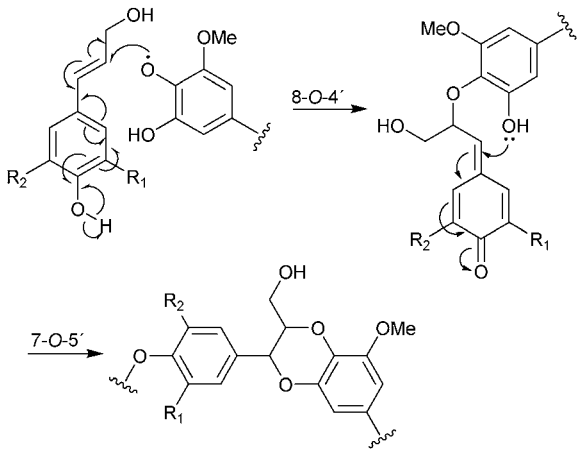

Fig. 9 Proposed formation of benzodioxane substructures in lignified vascular bundles (*mx* and/or *px*) *Arabidopsis* cell walls, and possibly *if* cell walls of the C4H::F5H transgenic line.

^{13}C NMR spectroscopic analysis of WT and C4H::F5H lignin enriched isolates for presence of benzodioxane substructures

To investigate the question of possible benzodioxane substructure formation during programmed lignification in the C4H::F5H line, it was next instructive to examine both WT and C4H::F5H lignin-enriched preparations using ^{13}C and 2D heteronuclear multiple quantum coherence (HMQC) NMR spectroscopic analyses. Analysis of the oxygenated carbon resonances in the aliphatic region (50–90 ppm)[31–33] from the WT lignin-enriched preparation (Fig. 10a) showed they contained all five expected H, G, S and G/S substructures (Fig. 10c, **I**–**V**), as assigned through their characteristic one-bond carbon–proton correlations (δ_C/δ_H): *i.e.* 60.7/3.12 and 60.7/3.47 (C9/H9), 84.1/4.18 (C8/H8) and 71.8/4.68 (C7/H7) ppm for 8-*O*-4′ aryl ether substructure **I**; 71.7/3.71 and 71.7/4.08 (C9/H9, C9′/H9′), 53.9/3.04 (C8/H8, C8′/H8′) and 85.6/4.58 (C7/H7, C7′/H7′) ppm for resinol-like substructure **II**; 63.4/3.69 and 63.4/3.41 (C9/H9), 53.6/3.39 (C8/H8) and 87.4/5.42 (C7/H7) ppm for phenylcoumaran substructure **III**; 62.3/4.03 and 62.3/3.94 (C9/H9), 85.7/4.07 (C8/H8) and 83.8/4.68 (C7/H7) ppm for dibenzodioxocin substructure **IV**, as well as 62.8/4.16 (C9/H9) ppm for cinnamyl alcohol end groups (**V**).

In contrast to WT, analysis of the HMQC NMR spectrum of the C4H::F5H lignin-enriched isolate (Fig. 10b) established the presence of an additional substructure that was characteri-zed by two correlations (δ_C/δ_H) at 76.2/4.87 (C7/H7) and 78.4/4.1 (C8/H8) ppm and consistent with a benzodioxane substructure **VI**.[34] No evidence for substructure **VI** was, however, obtained down to baseline detection under the conditions employed in the WT spectrum (Fig. 10a). Additionally, in contrast to the WT line (Fig. 10a), the resonances at 63.4/3.69 and 63.4/3.41 (C9/H9), 53.6/3.29 (C8/H8) and 87.4/5.42 (C7/H7) ppm for the phenylcoumaran substructure (**III**, Fig. 10c) were apparently absent as such in the C4H::F5H 2D HMQC NMR spectrum (Fig. 10b). NMR spectroscopic analysis of the HMQC cone volume of C7/H7 correlations at 71.8/4.68 and 76.2/4.87 ppm for the 8-*O*-4′ (**I**) and benzodioxane (**VI**) substructures, respectively, tentatively suggests that substructure **VI** may contribute to $\leq$15% of the overall 8-*O*-4′ interunit linkages present in the C4H::F5H lignin-enriched isolate.

Discussion

The findings herein have broad, general, implications for improving our overall understanding of macromolecular lignin assembly and configuration, the salient details of which are summarized below. These, in turn, may begin to provide new insight for the potential of lignin modification (composition/content) for improved biomass utilization for biofuels/bioproducts, *etc.*

Vascular development/lignification

Early phase. The *earliest* stage of "bolting stem" vascular apparatus development results primarily in *px* generation, with, for example, an ~6% putative lignin deposition in the WT line (Table 1). Manipulation of both *p*C3H and F5H activities, however, apparently had no significant influence though on the monomeric composition of the components laid down at this developmental stage in the different mutated/down-regulated lines (data not shown). This provisionally suggests that this early stage of vascular apparatus development is conserved and unaffected by such manipulations, even though use of the C4H promoter might have been anticipated to result in F5H hydroxylation of, for example, H and/or G moieties at C-3/C-5, respectively. Additionally, its provisional classification as "lignin" is uncertain, given that proteomic analyses indicated that an operational monolignol biosynthetic pathway was largely if not completely absent (data not shown).

This early phase of vascular development may be of additional importance given that all manipulations of the monolignol-forming pathway thus far have *NOT* resulted in abolition of *putative* lignification. Amongst the lowest levels achieved, these include those for *p*C3H manipulations (~62% lignin reduction estimates). This suggests that what is currently considered as the initial stages of lignification may involve distinct genes/enzymes and possibly intermediates, *i.e.* as far as estimates using current lignin analysis protocols (Klason lignin and acetyl bromide lignin estimates) are concerned.[1] This again underscores the urgent necessity to develop methodologies to fully characterize the precise chemical nature (*primary* structure(s)) of all of the polymeric entities/molecular species being generated at this stage, *i.e.* since 94–98% of this putative lignin cannot yet be accounted for by these degradative methodologies (see Table 1 and Fig. 5). Accordingly, what is truly being formed during this early phase of vascular development must await an improved (chemical/biochemical) understanding.

H-lignin enriched phenotype (*ref8* and alfalfa *p*C3H-I lines)

From the above analyses, it was not possible to conclude if the severely dwarfed, lignin-reduced (~62%) *p*C3H mutant resulted mainly from an inability to compensate for the constitutive allocation of carbon into the G and S monolignol-forming pathway. Alternatively, the mutant was so developmentally delayed, due to pleiotropic effects that essentially only the earliest stages of H-lignin deposition occurred. These

 This journal is © The Royal Society of Chemistry 2010

View Online

Downloaded by University of Tennessee at Knoxville on 05 August 2011
Published on 10 December 2009 on http://pubs.rsc.org | doi:10.1039/B819206E

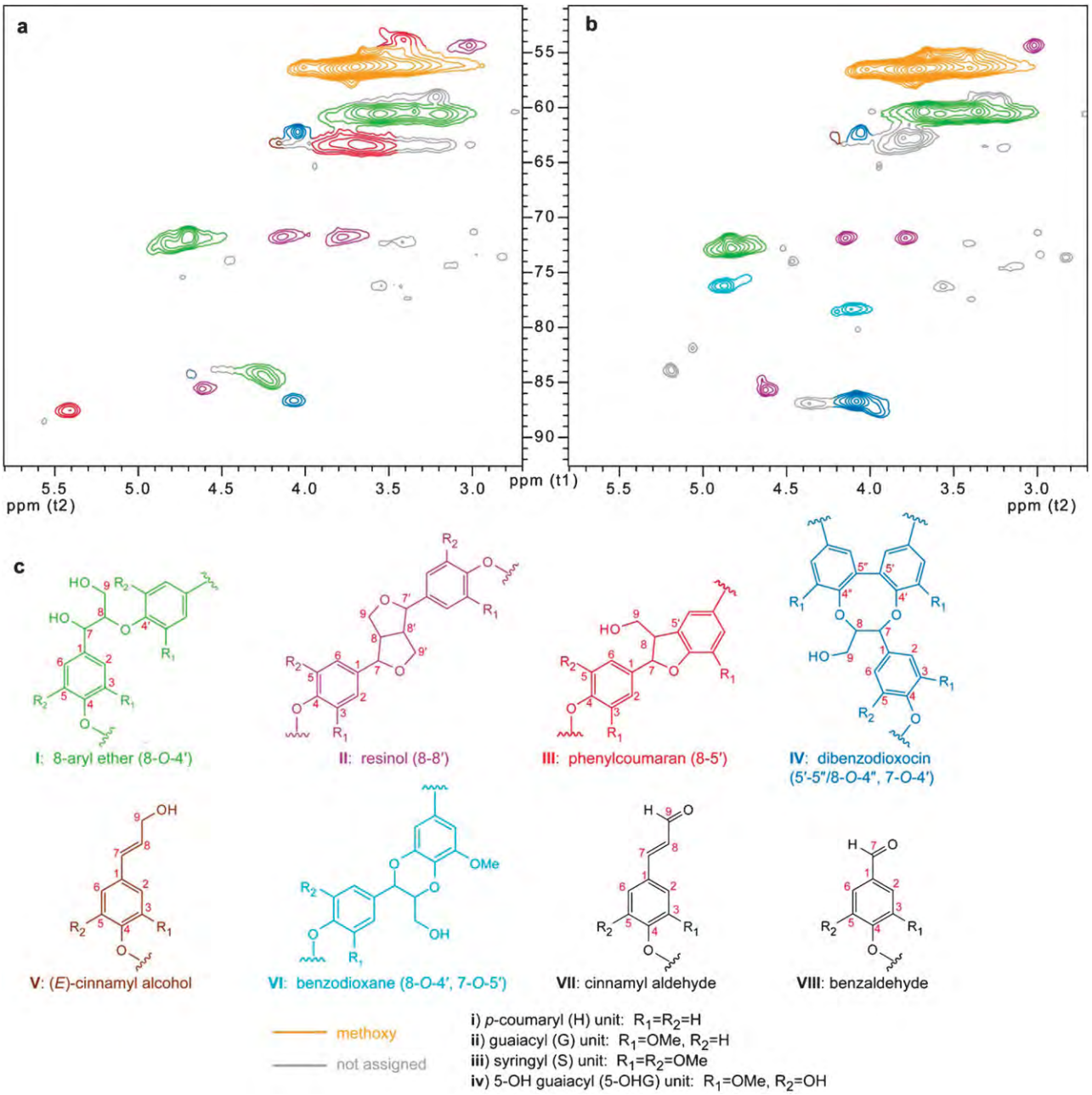

Fig. 10 HMQC spectra of oxygenated aliphatic region of lignin-enriched isolates from both wild type WT and C4H::F5H *Arabidopsis* (8 weeks; *stage 3* of reproductive growth[20]); (a) lignin-enriched isolate from WT; (b) lignin-enriched isolate from C4H::F5H; (c) lignin substructures as observed by NMR spectroscopic analyses.

pleitropic effects differed though from a *p*C3H down-regulated alfalfa line.[35] While also displaying essentially comparable levels of lignin reduction with an H-enriched phenotype, the alfalfa line, *p*C3H-I, showed little adverse effect on overall growth/development. Flowering, however, was delayed thus reducing reproductive potential. The underlying reasons for these growth/developmental differences in the two *p*C3H modulated lines (*Arabidopsis* and alfalfa) are as yet unknown.

From the *ref8* analyses, as well as that of the *p*C3H down-regulated alfalfa line[35] (Jourdes *et al*., manuscript in preparation), three important points could, nevertheless, be made.

Differential control over carbon allocation for H *vs*. G(S) lignin formation cannot readily be bypassed

The *Arabidopsis ref8* and the most extensively down-regulated alfalfa line (*p*C3H-I) gave comparable results in terms of both gross reductions in G/S lignin contents and slightly enhanced levels (~3–11 fold) of readily cleavable H-derived monomeric moieties at maturity, relative to that of fully lignified control (WT) tissues (Table 1). However, in *ref8*, the overall alkaline NBO-cleavable H-monomeric levels were more than 4-fold lower than the total amounts of H, G and S monomers released from WT lignins at maturation. This is interpreted

View Online

Downloaded by University of Tennessee at Knoxville on 05 August 2011
Published on 10 December 2009 on http://pubs.rsc.org | doi:10.1039/B819206E

as indicative of a rather directed, but essentially unplastic, form of metabolic control. That is, the presumed H-phase of constitutive lignification occurs first,[36] followed at best by a very limited ability for H-monomers to continue to be formed and to penetrate the G(S) macromolecular lignin-forming domains.

As noted aforehand, this lack of compensatory metabolic plasticity was suggested from results of autofluorescence microscopy and histochemical analyses. Lignin deposition mainly predominated in the *cwc*/*cml*, *i.e.* the considered sites of H-lignin deposition, with smaller amounts of H-monomers apparently partially extending into normal G(S) domains. The latter possibly represent a futile attempt to preserve lignification in these cell wall layers until H-monomer formation was either terminated or aborted.

Significantly though, relative to WT lines, the small increase in cleavable H-monomers in the *p*C3H mutated/down-regulated plant lines seems to be an attempt to duplicate, in terms of 8-*O*-4′ interunit linkage frequency, those typically found in the G/S lignins for an equivalent level of lignin deposition (see Table 1). This relatively small "penetration" of H-moieties into such domains provides no new insight, however, as to how lignin macromolecular configuration is being effectuated and controlled.

These findings also suggest that differential control of H *vs.* G/S lignin assembly is not readily by-passed. This is in agreement with our earlier metabolic flux studies which indicated differential control over carbon allocation to different branches of the H and G monolignol forming pathways.[15,37] Furthermore, monolignol **1***cannot readily* substitute for monolignols **2** and **3**, during the later *constitutive* phases of lignin formation in the normal G/S domains of the cell-walls, at least under these conditions. This, in turn, raises interesting questions as to the nature of the regulatory machinery operative in lignifying cells that ultimately prohibits over-production of the H-monomers, and thus of how this might be overridden. It also raises the question as to whether this apparently limited ability of the H-monomers to extend into the G/S domains is a metabolic checkpoint, *e.g.* as a sort of "buffering" effect to prevent any dislocation between the H and G(S) lignin domains should formation of the latter be slightly attenuated. It has also long been known that in gymnosperm compression wood lignin there is a higher H-content than in normal wood; modulation of monolignol biosynthesis in this way is envisaged to help contribute to different biophysical properties in the so-called "compression wood" and "normal wood", respectively.[38]

Preliminary studies by Franke *et al.*[19] had concluded that the *ref8* mutant "provides further support for plasticity in lignin biosynthesis". This was echoed by Ralph *et al.*[9] who stated that "such plants again illustrate the incredible metabolic plasticity of the lignification process", while also concluding that the *ref8* mutant "was totally devoid of the normal guaiacyl and syringyl units".

As evidenced from the study of *ref8*, this was not substantiated in either this or previous analyses of alfalfa *p*C3H down-regulated tissues[35] (Jourdes *et al.*, manuscript in finalization). All lines retained some G/S lignin forming capacity, although whether this results from residual *p*C3H activity, or *via* action of a different *p*C3H and/or polyphenol oxidase, for example, currently remains unknown. If "incredible metabolic plasticity" was operative when the G/S monolignol-forming pathway was largely blocked, why then was the lignin not fully formed in the cell-walls through replacement with equivalent amounts of the corresponding H-monomer? In spite of the metabolic "onslaught" imposed by *p*C3H manipulation, the biochemical response of the *Arabidopsis ref8* and alfalfa *p*C3H-I lines was remarkably unplastic as regards overall lignification.

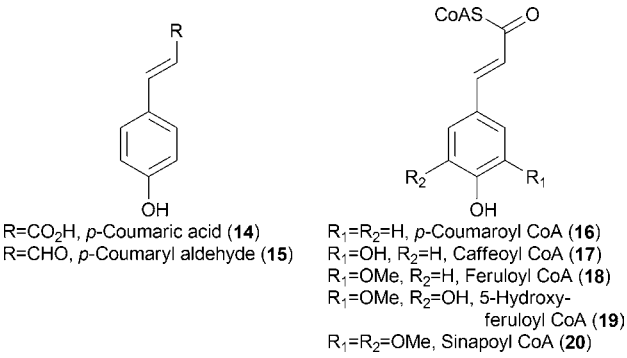

Intracellular control of monolignol formation

Franke *et al.*[19] indicated that reasons for the overall reduction in lignin content in *ref8* were unclear, and suggested the monolignol pathway enzymes were suboptimal for *p*-coumaryl alcohol (**1**) formation. This seems unlikely based on our more recent results using *Arabidopsis*. Comprehensive analyses of kinetic properties *in vitro* of these enzymatic steps using various *Arabidopsis* recombinant 4-coumarate CoA ligase (4CL),[39] cinnamoyl CoA reductase (CCR)[17] and cinnamyl alcohol dehydrogenase (CAD)[40] isoforms demonstrated that they quite effectively utilize *p*-coumaric acid (**14**), *p*-coumaroyl CoA (**16**) and *p*-coumaryl aldehyde (**15**), respectively. Indeed, for the various 4CLs characterized, *p*-coumaric acid (**14**) was one of the best substrates tested,[39] as was *p*-coumaryl aldehyde (**15**) with the CADs.[40] The *Arabidopsis* CCR1, by contrast, had K_{cat} values (s^{-1}) for *p*-coumaroyl CoA (**16**) [and caffeoyl CoA (**17**)] that were roughly an *order* of magnitude lower than that observed when using either feruloyl (**18**), 5-hydroxyferuloyl (**19**) or sinapoyl (**20**) CoAs.[17] Whether this reflects suboptimal formation of H-monolignol **1** therefore seems doubtful. Furthermore, our previous metabolic flux analyses using pine cell suspension cultures did not appear to indicate that the pathway to monolignol **1** was suboptimal in any critical way.[15,37]

*p*C3H modulation introduces structural defects which compromise overall composite strength properties, but not organismic survival, within a controlled environment

The physiological functions of macromolecular lignins are to provide structural support to soft tissues, as well as in helping form a conduit for water/nutrient conduction. Therefore, reductions in presumed lignin contents by up to ~62% through the *p*C3H mutation introduced significant defects in cell-wall structural integrity. This was most readily observable in the primary metaxylem regions of the *ref8* where

 This journal is © The Royal Society of Chemistry 2010

View Online

Downloaded by University of Tennessee at Knoxville on 05 August 2011
Published on 10 December 2009 on http://pubs.rsc.org | doi:10.1039/B819206E

considerable collapse of the vascular apparatus was evident. The *ref8* was unable to adequately compensate for loss in capacity of lignin formation and survives only in a defective, impaired, weakened state. If *true* metabolic plasticity had occurred, other (biochemical) processes would have been sufficiently "plastic" or robust to restore, for example, WT tissue mechanical properties.

This did not happen. Indeed, there is growing evidence indicating that modulation of macromolecular lignin amounts and/or composition introduces various structural defects into the vasculature, *i.e.* with accompanying significant reductions in overall mechanical strength robustness and cell-wall structural integrity.[1,2,16,35,41,42] This is *not* an example of metabolic plasticity. The organism has adapted only to the loss of its integral (physiological) functions as best it could when the G/S segments of lignin deposition are essentially unable to be formed.

Deficits introduced by *p*C3H modulation in *Arabidopsis* simply enable this organism to survive under the growth conditions experienced in a highly protective environment, such as in greenhouses/growth chambers. We currently have little definitive insight though into what effects such deficits will have on plant performance under various environmental (stress) conditions in the field, *e.g.* including effects of climatic changes on load-bearing capacity, encroachment by pathogens, and/or other stresses. The data thus far are only indicative of inabilities to adequately compensate for reductions in lignin amounts and to restore structural integrity of WT lines by any means. This is apparently not very different from what occurs with impaired bone formation, *i.e.* as often shown through changes in properties of Type 1 collagen or mineralized calcium phosphate (hydroxyapatite), and which can lead to increased skeletal fragility.[43,44]

The observations and interpretations made above thus run counter to views that "perfectly viable plants are obviously produced when blocking their enzymes and inhibiting the production of crucial monomers forces them to make lignins from abnormal precursors".[45] Perfectly viable plants were *not* being produced.

G-lignin-enriched phenotype

In the *fah* 1–2 plant line, the overall process of plant growth/development and lignification appears to be very similar to that for WT, with the exception that S-monomer formation was greatly reduced. This was demonstrated from histochemical staining and thioacidolysis/alkaline NBO analyses, as well as by pyrolysis GC/MS of the vascular bundles and inter-fascicular fibers, respectively. The pyrolysis GC/MS data strongly indicated that a G-enriched lignin was now present in both *xf*/*if* of the vascular bundles and the *if* cell walls, rather than having the S-enriched lignin present in both cell wall types of WT. That is, since the fiber-forming cell types can also apparently produce H/G-derived lignins to some extent, the overall effect of F5H mutation may have no adverse effect on overall programmed macromolecular lignin assembly and configuration. These data are thus generally consistent with the histochemical/autofluorescence microscopy analyses, which also suggested the absence of S-residues due to the F5H mutation.

Additionally, there was a relatively small increase in putative lignin amounts, as well as cleavable monomers released, per gram CWR in *fah* 1–2 relative to the WT line. If correct, this may reflect a slightly higher monomer packing density in the fiber-derived lignin, *i.e.* due to presence of the smaller G monomers rather than S moieties.

S-enriched phenotype

The C4H::F5H line resulted in a very distinct phenotype from that observed for either WT or *fah* 1–2. The reasons for these growth/developmental changes/differences are again not yet understood. Significantly, the overall increases in amounts of S-moieties in the C4H::F5H line, as suggested by histochemical staining, were apparently restricted to the *if* and *xf* cell types, *i.e.* those that typically engender formation of the S-enriched lignins (as well as smaller amounts of H and G).

The Mäule reagent detection of S-lignin in the *Arabidopsis* *xf* cell walls of the C4H::F5H line (Fig. 2) was an important point of anatomy not recognized by Meyer *et al.*;[8] they had incorrectly described S-lignin deposition as restricted to sclerified parenchyma that flank the vascular bundles (*i.e.* the *if* cells). The *xf* cell walls are though an additional constitutive site of S-lignin deposition within the vascular bundles. Thus, while our results in part agree with Meyer *et al.*,[8] in that 'some' tracheary elements failed to stain with the Mäule reagent, evidence is provided herein that disproves their claim of S-lignin deposition tissue-specificity being abolished by F5H over-expression. Indeed, our *xf*/*if* histochemical results (and pyrolysis GC/MS results, discussed below) indicated that S-lignin formation was essentially occurring only in both *xf*/*if* fiber cell wall types, albeit to presumably differing amounts, *i.e.* in the cells normally forming S-lignins. S-lignin formation was not detected in either the *px* or *mx*; these cells are *not* known to form S-lignins.

Pyrolysis GC/MS of *if* tissues from both C4H::F5H and WT clearly demonstrated that S-lignin was biosynthesized to a much larger extent relative to WT (see Fig. 7). These cell types are, however, constitutively able to at least partially synthesize S-lignins. By contrast, the vascular bundles from both WT and C4H::F5H tissues gave pyrograms which were apparently nearly identical in terms of profiles of H, G and S aromatic moieties (Fig. 8a and c). This was further support that S-lignin tissue specificity had not been abolished.

A previous study by Marita *et al.*[46] of the NMR spectroscopic analysis of a lignin-enriched isolate from the C4H::F5H line specifically disclosed that it was S-enriched and composed of almost entirely 8-*O*-4′-ether inter-unit linkages. If this were the case, however, it might have been anticipated that significantly higher levels of monomeric S-units—relative to those released in the *fah* 1–2 and WT lines—would have been cleaved/released upon thioacidolysis/alkaline NBO. However, no significant increase in cleavable monomeric moieties was observed in these analyses. That is, for example, the thioacidolysis monomer yields as a function of estimated/putative lignin contents were 26% (WT), 27% (*fah* 1–2) and 26% (C4H::F5H), respectively (Table 1). In an analogous manner, using alkaline NBO the monomers recovered were 28% (WT), 27% (*fah* 1–2) and 28% (C4H::F5H). It is

View Online

Downloaded by University of Tennessee at Knoxville on 05 August 2011
Published on 10 December 2009 on http://pubs.rsc.org | doi:10.1039/B819206E

estimated by NMR analyses (Fig. 10b) though that a small amount of benzodioxane (modified 8-*O*-4′) substructures (**VI**, Fig. 10c) was present in the lignin-enriched sample, isolated from the C4H::F5H line, this perhaps accounting for ≤15% of the 8-*O*-4′ interunit linkages.

These data provisionally suggest that in the vascular bundles, the *mx* or *px*/*mx* cells can form benzodioxane substructures. Of these, the *mx* cells are perhaps more likely, given the stronger level of histochemical staining for G moieties. This, in turn, would require that F5H is also being expressed in these particular cell types. The benzodioxane substructure would presumably be formed because the corresponding COMT is not expressed in either cell types, with COMT being responsible *in vivo* for the single methylation steps leading to constitutive S-monolignol (**3**) formation in fiber cells. It is thus assumed that F5H overexpression in these cell types is partly converting coniferyl alcohol (**2**) into 5-hydroxyconiferyl alcohol (**4**) in these cell types as discussed earlier.[2] To resolve this question, however, new chemistries will have to be developed at the single cell level to probe the nature of the lignin biopolymer(s) being formed in each cell type.

The data with the WT, *fah* 1–2, and C4H::F5H lines further support our previous observations[2] that carbon allocation for G/S (and 5-OHG) monomer supply during G/S (and 5-OHG) lignification is apparently not influenced by modulation of the G(S) segment of the lignin pathway, *i.e.* through alteration of G, 5-OHG and S ratios. This is consistent with our previous metabolic flux studies that indicated overall control of carbon allocation in the monolignol-forming pathway was spread over Phe availability, C4H (cinnamate-4-hydroxylase) and *p*C3H activities.[15,37] Carbon allocation to G, 5-OHG and S monolignol deposition, however, differs markedly from that for the H-monomers given the clear dislocation in compensatory H-monomer supply observed when G/S monomer formation was greatly attenuated. By contrast, carbon allocation to the G, 5-OHG and S segments appeared to be essentially unchanged regardless of modulations in monomer ratios.

Considered together, the data for the current study begins to provide further insight into lignin macromolecular assembly/configuration and the physiological consequences thereof of modulating same. For example, it was noted that COMT modulation—now known to result in benzodioxane substructure formation—leads to stem brittleness. This, in turn, begins to help explain the physiological effects of modulation of the various lignin (sub)structures in specific cell wall types and subcellular layers.

Limited substrate degeneracy, lignin primary structures, and proposed template replication

The limited substrate degeneracy (H *vs.* G *vs.* 5-OHG *vs.* S) has established that macromolecular lignin assembly(ies) within the various plant cell wall types and layers is (are) subject to significant constraints. For example, the amounts of releasable H, G, and S monomeric moieties were directly proportional and comparable for a given estimated lignin content. That is, there was a near invariance in (presumed) 8-*O*-4′ interunit linkage frequency (including that of benzodioxane substructures) within the different lignins of the distinct plant lines. This occurred irrespective of methoxyl/hydroxyl group substitution levels[1,16,17] (Jourdes *et al.*, manuscript in finalization). This is an important observation since the invariance of 8-*O*-4′ inter-unit linkages with methoxyl group substitution would not be expected if random coupling were occurring. The H, G and S monomers have 5, 4 and 3 positions available, respectively, for radical–radical coupling and would thus be anticipated to give different 8-*O*-4′ linkage frequencies if random coupling were occurring. However, the invariance of 8-*O*-4′ inter-unit linkages in these lignins *within the same plant species* is indicative of biochemical control over linkage placement/frequency.

We consider this as further indication that specific well-defined lignin primary structures are being generated. This has also been suggested from the use of various lignin antibodies (detecting distinctive substructures) with WT stem cross-sections.[47–50] These earlier studies resulted in differential detection of distinct lignin macromolecular substructures within specific cell wall layers/regions. Such documented changes are again consistent with biochemical control over lignin primary structure/macromolecular configuration(s) in for example, different cell wall layers.

Conclusions

From this study, several potentially important additional insights as regards programmed constitutive lignification have emerged in terms of lignin assembly and macromolecular configuration. These include: differential control over carbon allocation to different "segments" of the lignin pathway; current limitations in estimations of lignin contents and compositions; differences between "early" and "late" phases of putative lignification; limited substrate degeneracy, lignin primary structures, and proposed template replication.

Yet there still remain enormous gaps in the understanding of lignin assembly and lignin macromolecular configuration. Indeed, it must be emphasized that the study of both lignin (primary structure) proper and plant cell wall formation is essentially only beginning, as we are just now developing tools to probe same and establish what lignification is and how it occurs *in vivo*. There are numerous questions that need to be resolved: For example, the analytical chemistries available for the study of lignins are still at an unacceptable level, and new chemistries urgently need to be developed in order to quantify, for example, all linkage types. Additionally, following presumed monomer-monomer radical coupling, how do the growing lignin (primary) chains become re-oxidized at sites considered quite far removed from the oxidative enzyme active site(s) in the plant cell wall, *i.e.* so that radical-radical coupling with presumed incoming monomers can continue to occur? This is true not only for assembly of the presumed progenitorial lignin template(s) but also for the presumed template polymerization process which follows. Much work also remains to be done to probe and determine lignin primary structures, and how the biophysical properties of the cell wall are modulated by monomer replacement. This, in turn, emphasizes the urgent need to further establish all of the proteinaceous/enzymatic machinery involved in lignin macromolecular

 This journal is © The Royal Society of Chemistry 2010

View Online

Downloaded by University of Tennessee at Knoxville on 05 August 2011
Published on 10 December 2009 on http://pubs.rsc.org | doi:10.1039/B819206E

assembly/configuration, *i.e.* monomeric polymerization, mode of linkages, and conformations. The data, to date, suggest highly conserved processes, and do not apparently support other views that there may be no two lignin polymers that are identical in all plants![9] The data herein, and that from other analyses,[16,17] (Jourdes *et al.*, manuscript in finalization) do not support such a viewpoint.

Experimental

Plant materials and plant phenotype/growth analyses

Arabidopsis thaliana (L) Heynh (ecotype Columbia) wild type (WT), *ref8*, *fah* 1–2 and C4H::F5H transgenic lines, were cultivated as previously described.[17] Width and length measurements of the main bolting stems were taken using 20 individual plants every two days between 3 and 6 weeks post seed sown, after which growth/development had leveled off (see Fig. 1).

Morphological and histochemical studies

General anatomy was examined using fresh hand-cut sections from the base of the stem influorescence that had reached late *stage 2* of reproductive growth (according to the anatomical description by Altamura *et al.*[20]) for WT, *fah* 1–2 and C4H::F5H. Sections were stained with 1% Stevenel's Blue aq.[51,52] for 2 min, rinsed with distilled water and mounted on glass slides. For the *ref8*, stem tissue was used from plants that had also appeared to reach *stage 2*.[20] The *ref8* stem tissue was resin-embedded due to the fragility of its very small stems, which yielded poor hand-cut sections but responded well to resin treatment. For fixation, fresh tissue was trimmed to 3 mm in length, fixed in 2% paraformaldehyde and 1.25% glutaraldehyde in 50 mM Pipes buffer (pH 7.2) for 30 min at 25 °C. Tissues were then individually rinsed three times in this buffer for 10 min each, followed by dehydration using a standard ethanol series. Tissues were gradually embedded in medium grade L.R. White resin (London Resin, Co.) and heat polymerized at 60 °C overnight. Semi-thin sections were cut at 1 μm using a glass knife mounted on a Reichert-Jung ultramicrotome (Germany). Sections were dried onto gelatin-coated slides, stained with Stevenel's Blue[51,52] for 30 s, rinsed, dried and mounted in immersion oil. General anatomy light micrographs were recorded using an Olympus BH-2 photomicroscope equipped with a ProgRes C12plus digital microscope camera (JENOPTIK, Jena, Germany), except for the *ref8*, which was imaged using an Olympus microscope camera and Fujichrome 64T film.

Lignin histochemistry was examined using fresh hand-cut stem tissues from the same samples used for general anatomy (described above) for WT, *fah* 1–2, and C4H::F5H (see Fig. 3e–j), as well as from plants that were 2 and 4 weeks older, corresponding to late stage 2 and stage 3 of reproductive growth (data not shown). It was not possible to obtain good quality hand-cut sections from the *ref8* line due to its diminutive size and fragility when exposed to the lignin histochemical reagents. The Wiesner reagent (phloroglucinol-HCl)[22] was employed to detect G lignin (red color *via* reaction with presumed coniferaldehyde end-groups)[53–55] as described in Ruzin[21] and Patten *et al.*[17] The Mäule reagent[24] was used to detect S lignin (dark red histology)[27,54,56] in fresh hand-cut stem tissues as described in Chapple *et al.*[57] and Patten *et al.*[17] Histochemistry micrographs were recorded using an Olympus BH-2 photomicroscope fitted with a ProgRes C12plus digital microscope camera (JENOPTIK, Jena, Germany). Closeup inserted images of Fig. 2h and j were generated by cropping the high resolution file of the larger image to the regions of interest using Adobe Photoshop CS2 (Adobe Systems Inc., San Jose, CA, USA).

Lignin initiation and patterns of deposition

For the autofluorescence study, stem tissue was sampled at early lignification of both metaxylem and fiber cells, *i.e.* early *stage 2* of reproductive growth.[20] Tissue was embedded in L.R. White resin as described for general anatomy (above). Unstained resin sections were examined for autofluorescence of cell wall phenolics using a Leitz Aristoplan photomicroscope as described by Franceschi *et al.*[52]

Protoxylem imaging

Images of examples of protoxylem (*px*) tissues used (Fig. 4) were taken using hand-cut, unstained, sections of *Arabidopsis* WT inflorescence stems undergoing elongation that were ~1 cm or less in height (*i.e.* prior to anthesis of the first flower[20]). As before, images were recorded using a ProgRes C12plus digital camera (JENOPTIK, Jena, Germany) attached to an Olympus BH-2 photomicroscope. Fig. 4b is the product of thirty-four serial images to produce a single good resolution image of longitudinal protoxylem elements using Helicon Q1 Focus Lite software (Helicon Soft Ltd., Kharkov, Ukraine). All images were cropped (using Adobe Photoshop CS2; Adobe Systems Incorporated, San Jose, CA, USA) to allow close-up views of the regions of interest.

Laser capture microdissection (LCM) and isolation of lignifying tissues

Fresh stem tissue samples of mature plants, *i.e.* *stage* 3[20] were collected from WT, *fah* 1–2 and C4H::F5H plants, immediately frozen in liq N_2 and later embedded in Tissue-Tek® O.C.T.™ compound (Miles, Inc., Elkhart, IN). These were then individually sectioned at 14 μm using a Cryocut 1800 microtome (Leica Microsystems, Deerfield, IL), with sections mounted on clean alcohol-dipped glass slides and stored at 4 °C for not more than 3 days. Individual sections were then rinsed twice with distilled H_2O for 10 min each time to remove the O.C.T., and after drying at 37 °C, were laser microdissected (P.A.L.M.® Microbeam System, P.A.L.M. Microlaser Technologies, Germany) to isolate the vascular (xylary elements) and interfascicular fiber (*if*) regions of interest. The dissected samples were next placed in distilled H_2O (50 μl), with individual tissue samples extracted twice for 12 h with H_2O–acetone (3 : 7, v/v) under constant shaking conditions at 25 °C, then dried *in vacuo*.

Images of representative laser microdissected tissues (as described above) (Fig. 7) were taken using an Olympus BH-2 photomicroscope and a ProgRes C12plus digital camera (JENOPTIK, Jena, Germany). In the case of Fig. 7c, the

View Online

Downloaded by University of Tennessee at Knoxville on 05 August 2011
Published on 10 December 2009 on http://pubs.rsc.org | doi:10.1039/B819206E

isolated vascular bundle was bent during collection and could not be fully flattened for imaging; instead the image shown was generated by the assemblage of sixteen stacked images to produce a single in-focus image using Helicon Q1 Focus Lite software (Helicon Soft Ltd., Kharkov, Ukraine). Images were converted to grayscale and cropped to reduce excess empty space using Adobe Photoshop CS2 (Adobe Systems Incorporated, San Jose, CA, USA).

Pyrolysis GC/MS of laser microdissected tissues

Microdissected tissues, individually excised from the vascular bundle and interfascicular fiber regions, were separately pyrolyzed for 4 s at 500 °C using a microfurnace pyrolyzer (PYR-4A:Shimadzu). The pyrolyzer was interfaced at 270 °C with a Shimadzu GC-17A gas chromatograph coupled to a Shimadzu QP-5000 mass spectrometer. Vapor phase products were separated on a XTI-5 capillary column (Rexdek, 30 m × 0.25 mm) using a 5 °C min^{-1} gradient beginning at 50 °C for 1 min, then programmed at 5 °C min^{-1} until 270 °C. Pyrolysis products were identified on the basis of comparison with authentic standards and/or with literature mass spectroscopic fragmentation data[28,29] as needed (Table 2).

Whole stem lignin chemistry (Klason and acetyl bromide, nitrobenzene oxidation and thioacidolysis analyses)

Stems from WT (approximately 400 at early bolting stage of 1 cm in height; *pre-anthesis*[20]), as well as 20 stem samples of WT, *fah* 1–2 and C4H::F5H lines at 7 weeks (*stage 3*[20]), were manually ground in liq. N_2 and lyophilized. Samples were then individually ball-milled for 1 h followed by successive extractions using EtOH–toluene (1 : 1, v/v), EtOH, and distilled H_2O,[17] respectively, with the extractive-free samples thus obtained dried *in vacuo*. Total Klason lignin estimations were carried out gravimetrically using the TAPPI test method (T222 om-88),[58] with soluble lignin measured in the filtrate by UV spectrophotometry at 205 nm and corrected using 110 g^{-1} cm^{-1} as the extinction coefficient.[59] AcBr analyses were conducted as described in Jourdes *et al.*[16] Alkaline NBO analyses were carried out with 30 mg samples,[60] with products analyzed using an HP6890 series gas chromatograph coupled to an HP 5973 mass detector.[61] Oxidized products were separated on a DB-5 column (30 m × 0.25 mm) using a temp. gradient from 140 °C to 250 °C at a rate of 2 °C min^{-1}, followed by a final 5 min hold at 250 °C. Ethyl vanillin was used as an internal standard for quantification/calibration. Thioacidolysis analyses[61] were carried out by treating 15 mg lyophilyzed samples with thioacidolysis reagent [20 ml, 0.2 M BF_3-etherate in dioxane–ethanethiol at 8.75 : 1 (v/v)]. Following thioacidolysis, samples were individually extracted with CH_2Cl_2 (20 ml × 3), with the combined extracts individually analyzed by GC/MS as described for alkaline NBO;[61] tetracosane was used as an internal standard for thioacidolysis.

NMR spectroscopic analyses of C4H::F5H and WT lignin-enriched isolates

The lignin-enriched isolates from WT (268 mg) and C4H::F5H (246 mg) plants were obtained by individually submitting the extractive-free CWRs (∼8 g) from 8-week old stems (*stage 3*[20]) of both lines to the Björkman lignin isolation procedure as described previously.[16] These isolates correspond to ∼17.2% (from WT) and ∼17.7% (from C4H::F5H) of the estimated AcBr lignins in the starting CWR. NMR spectra were recorded on a Varian Inowa 500 MHz spectrometer (Varian Inc., Palo Alto, CA, USA) at 325°K in DMSO-d_6 and referenced to a residual solvent signal at 2.49 ppm and 39.5 ppm for proton and carbon, respectively. The lignin-enriched isolates (∼30 mg) from both WT and C4H::F5H were dissolved individually in 500 μL of DMSO-d_6 (99.9% D, Sigma-Aldrich) for NMR spectroscopic analyses. ^{13}C NMR, two-dimensional phase-sensitive gradient-selected HMQC of lignin-enriched isolates from both lines (WT and C4H::F5H) were recorded individually using similar parameters, as described earlier.[62]

Acknowledgements

The authors thank the US Department of Energy (DE FG03-97ER20259), the US National Science Foundation (MCB-0417291), the BioEnergy Science Center, a US Department of Energy Bioenergy Research Center supported by the Office of Biological and Environmental Research in the DOE Office of Science, and the G. Thomas and Anita Hargrove Center for Plant Genomic Research for generous financial support. Dr Clint Chapple is gratefully acknowledged as the source of *ref8*, *fah* 1–2 and C4H::F5H seeds.

References

1 L. B. Davin, M. Jourdes, A. M. Patten, K.-W. Kim, D. G. Vassão and N. G. Lewis, *Nat. Prod. Rep.*, 2008, **25**, 1015–1090.
2 A. M. Anterola and N. G. Lewis, *Phytochemistry*, 2002, **61**, 221–294.
3 L. B. Davin, A. M. Patten, M. Jourdes and N. G. Lewis, in *Biomass Recalcitrance. Deconstructing the Plant Cell Wall for Bioenergy*, ed. M. E. Himmel, Blackwell Publishing, Oxford, UK, 2008, pp. 213–305.
4 A. M. Patten, A. M. Anterola, B.-Y. Chung, L. B. Davin and N. G. Lewis, *Fourteenth International Conference on Arabidopsis Research, Madison, WI, June 2003*.
5 A. M. Patten, C. L. Cardenas, D. D. Laskar, L. B. Davin and N. G. Lewis, *Annual Meeting: Phytochemical Society of North America, San Diego, CA, August 2005*.
6 G. Angeles, J. Berrio-Sierra, J. P. Joseleau, P. Lorimier, A. Lefèbvre and K. Ruel, *Planta*, 2006, **224**, 228–232.
7 N. G. Lewis and E. Yamamoto, *Annu. Rev. Plant Physiol. Plant Mol. Biol.*, 1990, **41**, 455–496.
8 K. Meyer, A. M. Shirley, J. C. Cusumano, D. A. Bell-Lelong and C. Chapple, *Proc. Natl. Acad. Sci. U. S. A.*, 1998, **95**, 6619–6623.
9 J. Ralph, K. Lundquist, G. Brunow, F. Lu, H. Kim, P. F. Schatz, J. M. Marita, R. D. Hatfield, S. A. Ralph, J. H. Christensen and W. Boerjan, *Phytochem. Rev.*, 2004, **3**, 29–60.
10 S.-Y. Guan, J. Mlynár and S. Sarkanen, *Phytochemistry*, 1997, **45**, 911–918.
11 S. Sarkanen, in *Lignin and Lignan Biosynthesis*, ed. N. G. Lewis and S. Sarkanen, ACS Symposium Series, Washington, 1998, pp. 194–208.
12 Y.-r. Chen and S. Sarkanen, *Phytochem. Rev.*, 2003, **2**, 235–255.
13 Y.-r. Chen and S. Sarkanen, *Proceedings of the 8th International Lignin Institute Forum, Rome, May 10–12*, 2007, pp. 1–4.
14 J. Ralph, G. Brunow, P. J. Harris, R. A. Dixon, P. F. Schatz and W. Boerjan, in *Recent Advances in Polyphenol Research*, ed. F. Daayf and V. Lattanzio, Wiley-Blackwell, 2008, pp. 36–66.
15 A. M. Anterola, J.-H. Jeon, L. B. Davin and N. G. Lewis, *J. Biol. Chem.*, 2002, **277**, 18272–18280.

 This journal is © The Royal Society of Chemistry 2010

View Online

Downloaded by University of Tennessee at Knoxville on 05 August 2011
Published on 10 December 2009 on http://pubs.rsc.org | doi:10.1039/B819206E

16 M. Jourdes, C. L. Cardenas, D. D. Laskar, S. G. A. Moinuddin, L. B. Davin and N. G. Lewis, *Phytochemistry*, 2007, **68**, 1932–1956.
17 A. M. Patten, C. L. Cardenas, F. C. Cochrane, D. D. Laskar, D. L. Bedgar, L. B. Davin and N. G. Lewis, *Phytochemistry*, 2005, **66**, 2092–2107.
18 R. Franke, J. M. Humphreys, M. R. Hemm, J. W. Denault, M. O. Ruegger, J. C. Cusumano and C. Chapple, *Plant J.*, 2002, **30**, 33–45.
19 R. Franke, M. R. Hemm, J. W. Denault, M. O. Ruegger, J. M. Humphreys and C. Chapple, *Plant J.*, 2002, **30**, 47–59.
20 M. M. Altamura, M. Possenti, A. Matteucci, S. Baima, I. Ruberti and G. Morelli, *New Phytol.*, 2001, **151**, 381–389.
21 S. E. Ruzin, *Plant Microtechnique and Microscopy*, Oxford University Press, New York, NY, 1999.
22 J. Wiesner, *Sitzungsberichte der Kaiserlichen Akademie der Wissenschaften. Mathematisch-Naturwissenschaftlichen Classe*, 1878, **77**, 60–66.
23 K. Esau, *Plant Anatomy*, John Wiley and Sons, Inc., New York, NY, USA, 1967.
24 C. Mäule, *Beiträge zur wissenschaftlichen Botanik*, 1901, **4**, 166–185.
25 J. F. D. Dean, *Methods Plant Biochem. Mol. Biol.*, 1997, 199–215.
26 R. D. Gibbs, in *The Physiology of Forest Trees*, ed. K. V. Thimann, W. B. Critchfield and M. H. Zimmermann, The Ronald Press Co., New York, NY, USA, 1957, pp. 269–312.
27 Y. Watanabe, K. Fukazawa, Y. Kojima, R. Funada, T. Ona and T. Asada, *Mokuzai Gakkaishi*, 1997, **43**, 102–107.
28 O. Faix, D. Meier and I. Fortmann, *Holz Roh- Werkst.*, 1990, **48**, 351–354.
29 O. Faix, D. Meier and I. Fortmann, *Holz Roh- Werkst.*, 1990, **48**, 281–285.
30 R. Atanassova, N. Favet, F. Martz, B. Chabbert, M.-T. Tollier, B. Monties, B. Fritig and M. Legrand, *Plant J.*, 1995, **8**, 465–477.
31 P. Karhunen, P. Rummakko, J. Sipilä, G. Brunow and I. Kilpeläinen, *Tetrahedron Lett.*, 1995, **36**, 169–170.
32 N. G. Lewis, J. Newman, G. Just and J. Ripmeister, *Macromolecules*, 1987, **20**, 1752–1756.
33 S. A. Ralph, J. Ralph and L. L. Landucci, Available at URL http://www.dfrc.ars.usda.gov/software.html, 2004.
34 J. Ralph, C. Lapierre, J. M. Marita, H. Kim, F. Lu, R. D. Hatfield, S. Ralph, C. Chapple, R. Franke, M. R. Hemm, J. Van Doorsselaere, R. R. Sederoff, D. M. O'Malley, J. T. Scott, J. J. MacKay, N. Yahiaoui, A. M. Boudet, M. Pean, G. Pilate, L. Jouanin and W. Boerjan, *Phytochemistry*, 2001, **57**, 993–1003.
35 A. M. Patten, M. Jourdes, E. E. Brown, M.-P. Laborie, L. B. Davin and N. G. Lewis, *Am. J. Bot.*, 2007, **94**, 912–925.
36 P. Whiting and D. A. I. Goring, *Wood Sci. Technol.*, 1982, **16**, 261–267.
37 A. M. Anterola, H. van Rensburg, P. S. van Heerden, L. B. Davin and N. G. Lewis, *Biochem. Biophys. Res. Commun.*, 1999, **261**, 652–657.
38 T. E. Timmel, *Compression Wood in Gymnosperms*, Springer-Verlag, New York, NY, USA, 1986.
39 M. A. Costa, D. L. Bedgar, S. G. A. Moinuddin, K.-W. Kim, C. L. Cardenas, F. C. Cochrane, J. M. Shockey, G. L. Helms, Y. Amakura, H. Takahashi, J. K. Milhollan, L. B. Davin, J. Browse and N. G. Lewis, *Phytochemistry*, 2005, **66**, 2072–2091.
40 S.-J. Kim, M.-R. Kim, D. L. Bedgar, S. G. A. Moinuddin, C. L. Cardenas, L. B. Davin, C. Kang and N. G. Lewis, *Proc. Natl. Acad. Sci. U. S. A.*, 2004, **101**, 1455–1460.
41 D. G. Hepworth and J. F. V. Vincent, *Ann. Bot.*, 1998, **81**, 751–759.
42 D. G. Hepworth and J. F. V. Vincent, *Ann. Bot.*, 1999, **83**, 39–43.
43 L. Bozec, J. de Groot, M. Odlyha, B. Nicholls, S. Nesbitt, A. Flanagan and M. Horton, *Ultramicroscopy*, 2005, **105**, 79–89.
44 J. L. Ferretti, G. R. Cointry, R. F. Capozza and H. M. Frost, *Mech. Ageing Dev.*, 2003, **124**, 269–279.
45 J. Ralph, *9th International Symposium on Wood and Pulping Chemistry*, 1997, **1**, 5–11.
46 J. M. Marita, J. Ralph, R. D. Hatfield and C. Chapple, *Proc. Natl. Acad. Sci. U. S. A.*, 1999, **96**, 12328–12332.
47 J. P. Joseleau and K. Ruel, *Plant Physiol.*, 1997, **114**, 1123–1133.
48 E. M. Kukkola, S. Koutaniemi, M. Gustafsson, P. Karhunen, K. Ruel, T. K. Lundell, P. Saranpää, G. Brunow, T. H. Teeri and K. V. Fagerstedt, *Planta*, 2003, **217**, 229–237.
49 G. Müsel, T. Schindler, R. Bergfeld, K. Ruel, G. Jacquet, C. Lapierre, V. Speth and P. Schopfer, *Planta*, 1997, **201**, 146–159.
50 K. Ruel, O. Faix and J. P. Joseleau, *J. Trace Microprobe Tech.*, 1994, **12**, 247–265.
51 M. del Cerro, J. Cogen and C. del Cerro, *Microsc. Acta*, 1980, **83**, 117–121.
52 V. R. Franceschi, T. Krekling, A. H. Berryman and E. Christiansen, *Am. J. Bot.*, 1998, **85**, 601–615.
53 E. Adler, K. J. Björkqvist and S. Häggroth, *Acta Chem. Scand.*, 1948, **2**, 93–94.
54 J. Nakano and G. Meshitsuka, in *Methods in Lignin Chemistry*, ed. S. Y. Lin and C. W. Dence, Springer-Verlag, Berlin, Germany, 1992, pp. 23–32.
55 F. Pomar, F. Merino and A. Ros Barcelò, *Protoplasma*, 2002, **220**, 17–28.
56 K. Iiyama and R. Pant, *Wood Sci. Technol.*, 1988, **22**, 167–175.
57 C. C. S. Chapple, T. Vogt, B. E. Ellis and C. R. Somerville, *Plant Cell*, 1992, **4**, 1413–1424.
58 C. W. Dence, in *Methods in Lignin Chemistry*, ed. S. Y. Lin and C. W. Dence, Springer-Verlag, Berlin, Germany, 1992, pp. 33–61.
59 A. G. Schöning and G. Johansson, *Sven. Papperstidn.*, 1965, **68**, 607–613.
60 K. Iiyama and T. B. T. Lam, *J. Sci. Food Agric.*, 1990, **51**, 481–491.
61 K. Blee, J. W. Choi, A. P. O'Connell, S. C. Jupe, W. Schuch, N. G. Lewis and G. P. Bolwell, *Phytochemistry*, 2001, **57**, 1159–1166.
62 D. D. Laskar, M. Jourdes, A. M. Patten, G. L. Helms, L. B. Davin and N. G. Lewis, *Plant J.*, 2006, **48**, 674–686.